2014-01-01

Design and Development of a High Velocity Oxy-Fuel Thermal Spray Gun

Luisa Alejandra Cabrera Maynez
University of Texas at El Paso, lacabrera@miners.utep.edu

DESIGN AND DEVELOPMENT OF A HIGH VELOCITY OXY-FUEL THERMAL SPRAY GUN

LUISA ALEJANDRA CABRERA MAYNEZ

Department of Mechanical Engineering

APPROVED:

Ahsan Choudhuri , Ph.D., Chair

Norman Love Jr., Ph.D.

Cristian Botez, Ph.D.

Charles Ambler, Ph.D.

Dean of the Graduate School

Dedication

I wish to dedicate this work to those in my family who have given me their unconditional love and support throughout my entire life. To the strongest person I know, my mother, thank you being the best role model I could ever ask for, and for helping me build the confidence and independence to follow my dreams as you have followed and achieved yours. To my grandparents and Aunt Sandra I wish to show gratitude for always having their arms open for comfort and care in the times I need it the most. To my brother, my first and best friend, I am grateful for loving me at my best and worst, and for making me see the humor in every little thing. Finally to my boyfriend Arifur, I want to thank for motivating me to be the best I can, and for always being there to provide his absolute support.

DESIGN AND DEVELOPMENT OF A HIGH VELOCITY OXY-FUEL THERMAL SPRAY GUN

by

LUISA ALEJANDRA CABRERA MAYNEZ, BSME

THESIS

Presented to the Faculty of the Graduate School of

The University of Texas at El Paso

in Partial Fulfillment

of the Requirements

for the Degree of

MASTER OF SCIENCE

Department of Mechanical Engineering

THE UNIVERSITY OF TEXAS AT EL PASO

August 2014

Acknowledgements

I would like to express my great appreciation for my committee chair Dr. Choudhuri, who has always provided his leadership and support throughout my academic career. I also wish to thank the professors involved in this project, namely Dr. Love and Dr. Ramana, who have given their time to deliver excellent mentoring and advice for my team. I take this opportunity to thank all faculty and staff in the Mechanical Engineering department as well as my colleagues in the cSETR laboratory, in particular my teammate Diaaeldin Mohamed, as this work would have not been possible without all their help. Financial support during this time was provided by the mechanical engineering department at the University of Texas at El Paso and the United States Department of Energy under award DEFG2612FE0008548. However, any opinions, findings, conclusions, or recommendations expressed herein are those of the authors and do not necessarily reflect the views of the U. S. Department of Energy.

Abstract

The High Velocity Oxy-Fuel (HVOF) system is a highly promising technique for the production of thermal barrier coatings (TBCs), helpful in the protection of materials exposed to extreme thermal and corrosive environments. Coatings generated through the technique are employed in industrial settings to extend product life, increase performance and decrease maintenance costs. HVOF yields lower porosity and higher adhesion TBCs when compared to similar thermal spraying processes. Though gas fuelled systems are the norm in this technique, there is a recent interest in employing liquids due to their low cost and increased deposit density. Economic and highly scalable, HVOF process optimization is key to the development of next-generation systems. The work presented in this investigation focuses on the design and manufacturing of a liquid-fuelled HVOF gun through the individual consideration of design aspects and test equipment components. A flammability investigation for gas is performed on the manufactured prototype; to accompany the study a CFD model is developed and presented for future comparisons. Further investigations on the subject and system will focus on the transition to liquid fuel in the model and the study of coating particle trajectories.

Table of Contents

List of Tables

List of Figures

Chapter 1: Introduction

All mechanical parts exhibit physical and chemical degradation ultimately resulting in failure through regular use. Techniques that slow or stop this degradation are constantly sought after and continuously innovated, particularly for use in new-generation power plants, whose operational parameters produce extremely harsh environments in terms of mechanical and thermal stresses. Boilers and turbines in these systems are particularly affected, as increased efficiency also brings extreme temperatures and corrosive environments.

A proposed solution to the issue exists in the form of thermal barrier coatings (TBCs). Thermal barrier coatings are complex, multifunctional films (with thicknesses ranging between 100 μm and 2 mm) of a refractory material that protects a substrate from extreme temperatures. (Clarke & Phillpot, 2005) TBCs generally consist of a metallic base, oxidation-resistant bond coat and a zirconia-based top coating, is sprayed on the former. Nanostructured coatings have proven to be an effective means to improve component characteristics, extend product life, increase performance and reduce production and maintenance costs (Li & Christofides, 2005).

TBCs allow for a greater increase in gas temperatures without raising the base metal temperature (Brandl, Toma, Kruger, Grabke, & Matthaus, 1997). Grain sizes below 100 nm are of special interest, as the properties of such powders are superior to conventional materials, including but not limited to improved strength, hardness, ductility and sinterability (Dongmo, Wenzelburger, & Gadow, 2008) (Li & Christofides, 2005). Nanostructured coatings are widely used in many industries to extend product life, increase performance as well as reduce production and maintenance costs; they are particularly employed to enhance fuel efficiency in internal combustion engines, which are subjected to severe working conditions in elevated temperatures (Jang, Park, Jung, Jang, Choi, & Paik, 2006).

Thermal spraying is one of the many existing techniques for the forming of TBCs. It is defined as a group of processes that use a heat source to melt coating materials while transferring kinetic energy to the particulates, using jets to propel molten particles towards a surface. When the hot particles impact the surface of the substrate (or piece to be coated), they solidify quickly; as subsequent particles impact the piece a deposit is built up (Davis, 2004).

Thermal energy for spraying processes may be generated chemically through combustion of fuels, or through the electrical heating of industry-supplied gases. One of the most practical means to produce kinetic energy needed to supply to the particles is through the use of a nozzle; a nozzle accelerates a gas stream and confines the particles to a specific path on the jet where they can be heated and propelled (Davis, 2004). Energy can be applied directly in the form of arc spraying, or indirectly through flame or plasma jets.

Although various coating techniques have been developed over the last few years, most significantly atomic plasma spraying (APS), vapor deposition and powder coating, the high velocity oxy-fuel (HVOF) technique has shown promise in TBCs due to its high performance characteristics in fossil power systems. It is regularly employed to deposit metallic alloys, composites and polymers to enhance durability and has been widely used in the automotive, aerospace and chemical industries (Tabbara & Gu, 2009) (Kamali & Binesh, 2009). HVOF is classified as part of thermal spraying processes; a summary of this method and other spraying technologies follows below.

1.1 Flame Spray Methods

Flame Spray

This technique uses combustion fuel gases to generate heat. The most common configuration is that of the oxyacetylene torch to generate highest temperatures through oxy-fuel combustion. It is compatible with a wide range of materials, including powders, wires or rods. In this conformation melted coating materials are accelerated towards a substrate through an expanding gas flow, aided also by air jets. In flame spray materials are introduced axially through the back part of the nozzle or directly into the flame at the nozzle exit. Speeds are below 100 m/s with particle impact velocities of about 80 m/s. Temperatures are kept above 2600 C, varied by changing combustion temperature through the arrangement of configurations and mixing patterns. Flame spray guns always run near stoichiometric conditions. The flame spray technique yields coating densities ranging from 85 to 98 percent depending on the specific technique and fuels used. A disadvantage of this method is the fact that it produces relatively coarse microstructures and high porosity levels.

Detonation Gun

Detonation guns produce high thermal & velocity jets by confining combustion within a tube or barrel into which the coating powder is introduced. This design produces a significant amount of heat and transfers a great amount of momentum to the powder particles. In this setup an explosive mixture of oxidizer, fuel and powder is introduced into a tube and ignited by a spark plug. The resultant pressure wave heats and accelerates the powder towards the substrate at a high frequency. Nitrogen is used as a purging agent in between runs. High particle velocities (above 800 m/s) are generated through this method; high kinetic energy helps to reduce or

completely eliminate porosity. Compared to conventional thermal spray, the detonation gun method produces finer, thinner splat features; this technique produces some of the densest and hardest of all sprayed materials, and it is regularly used for commercial aircraft engine coatings (Davis, 2004).

Electric Arc Spray

Electric arc spray technology uses a direct-current electric arc continuously struck between two consumable electrode rods to produce direct melting. The thermal efficiency of the electric arc spray process is quite high compared to other thermal spray techniques, as most of its heat is used for melting and particle deposition. A high-velocity air jet shears away the molten wires, breaking up the material into fine particles and creating a fine distribution of metal. Dwell time for the configuration must be shortened in order to minimize oxidation. The materials for the electric arc spray are limited to conductive constituents that can be reshaped into wire form. A variety of substrate materials can be used for this application due to the cooler characteristic of the arc spray (Davis, 2004).

Plasma Spray

A DC plasma arc gun combines an axially aligned cathode and anode. Water cooling constricts and stabilizes the arc and accelerates the expanding preheated gases. Plasma forming gases are introduced at the back of the gun; the gases enter the arc chamber through a ring that imparts a spin or vortex flow. The vortex stabilizes the arc at the cathode tip; powder is subsequently injected into the stream at the exit. The injection angles of the coating material determine particle final conditions. Jet exit temperatures exceed 12,000 C, making this the hottest thermal spray process. Resultant coatings can have porosity equal to that of the

detonation or HVOF processes, depending on material properties, gun geometry and overall configuration. An additional advantage of the process is the fact that the oxide content is the lowest among all thermal spray configurations (Davis, 2004).

High Velocity Oxy-Fuel (HVOF)

High Velocity Oxy-Fuel (HVOF) thermal spraying was developed in the 1930s and has been commercially available for two decades (Tabbara & Gu, 2009); it is considered to be a particularly promising technique due to its compatibility with a wide range of coating materials as well as its adjustable thickness coatings. Its fast deposition rate leads to high bond strength, hardness and wear resistance due to its homogeneous distribution of powder; in addition, the process is economic and highly scalable (Kamnis & Gu, 2006) (Tabbara & Gu, 2009). HVOF produces high-quality results comparable to those of detonation gun coatings, and provides a good control of residual stress (Davis, 2004). One example of the advantages of this process lies in the fact that HVOF has lower production costs than vapor deposition due to the fact that it does not require vacuum conditions (Brandl, Toma, Kruger, Grabke, & Matthaus, 1997). The HVOF technique employs a high temperature supersonic gas generated from oxy-fuel combustion to impinge high velocity particles upon a surface. The fuel-oxidizer combination is burned in a high pressure combustion chamber, where the mixture is combusted into complex gaseous products (Tabbara & Gu, 2009). Resulting gases are accelerated using a convergent-divergent nozzle to supersonic velocity; coating particles are injected either through the initial oxidizer line or fed through a carrier gas downstream (Tabbara & Gu, 2009) (Katanoda, Morita, Komatsu, & Kuroda, 2011) (Dongmo, Wenzelburger, & Gadow, 2008). Particles hit the substrate, cool and solidify, creating a thin layer of material (Li & Christofides, 2005). One of the main features of HVOF is its ability to propel powder at high velocities without overheating

or melting them, increasing their adhesion to both themselves and to the substrate resulting in a low-porosity bond coat (Tabbara & Gu, 2009) (Davis, 2004) (Dongmo, Wenzelburger, & Gadow, 2008). In a well-designed gun the maximum attainable gas velocity is 2000 m/s, reaching Mach 2 at the nozzle exit (Kamali & Binesh, 2009); in order to transfer as much kinetic energy as possible to the particles, the gas jet is usually maintained as supersonic outside the torch; this depends on the nozzle expansion conditions (Li & Christofides, 2005). Compared to plasma spraying, particle melting and oxidation rates are lesser due to lower overall temperatures (Dongmo, Wenzelburger, & Gadow, 2008) (Basu & Cetegen, 2008) (Li & Christofides, 2005); superheating or vaporization is prevented through an effective control of temperature. High particle momentum is a substitute for lower temperatures once the in-flight kinetic energy deforms the particles when hitting the substrate (Davis, 2004). Coatings produced by this system are denser and show better resistance to oxidation when compared to various alternate deposition methods. Although a wide range of materials are able to be used for HVOF coatings, the significantly lower temperature of the flame does not allow processing of high melting point ceramics and only limited success has been achieved in this matter (Basu & Cetegen, 2008).

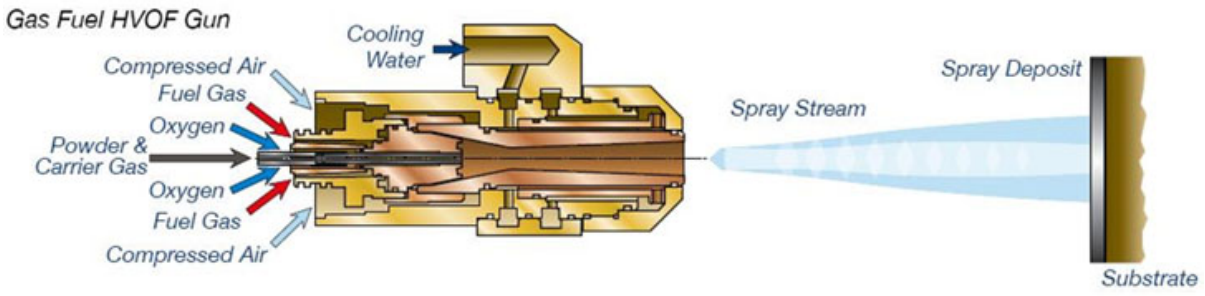

Figure 1.1 : General Schematic of a gaseous-fuelled HVOF gun

Powder particles for HVOF use range from 5 to 80 μm and have the capability to build coatings up to several mm in thickness (Tabbara & Gu, 2009). Particle types mainly consist of

alloys and superalloys, included but not limited to metals such as iron, aluminum, bronze and stainless steel. One alloy in particular, Inconel 718, has attracted recent interest due to its superior quality of coating density and excellent resistance to extreme environments (Singh Nalwa, 1999).

Since the physical and mechanical properties of HVOF sprayed coatings are strongly influenced by the nano or microstructure of the deposit, depending themselves on the physical and chemical states of the particles when impinging the substrate (temperature, velocity, melting degree, oxidants) (Li & Christofides, 2005) it is important to optimize design key process parameters (O/F ratio, gas flow rate, spraying distance, powder material) to ensure that one the best coating possible is produced.

Attribute	Flame spray	High-velocity oxyfuel	Detonation gun	Wire arc	Air plasma	Vacuum plasma	Radiofrequency plasma
Jet							
Jet temperature, K	3500	5500	5500	>25,000	15,000	12,000	10,000
Jet velocities, m/s (ft/s)	50–100 (160–300)	500–1200 (1600–4000)	>1000 (>3300)	50–100 (160–300)	300–1000 (1000–3300)	200–600 (700–2000)	20–80 (70–300)
Gas flow, sLm	100–200	400–1100	N/A	500–3000	100–200	150–250	75–150
Gas types	O_2, acetylene	CH_4, C_3H_6, H_2, O_2	O_2, acetylene	Air, N_2, Ar	Ar, He, H_2, N_2	Ar, He, H_2	Ar, He, H_2
Power input, kW equiv.	20	150–300	N/A	2–5	40–200	40–120	40–200 (plate)
Particle feed							
Particle temperature (max), °C (°F)	2500 (4500)	3300 (6000)	N/A	>3800 (>6900)	>3800 (>6900)	>3800 (>6900)	>3800 (>6900)
Particle velocities, m/s (ft/s)	50–100 (160–300)	200–1000 (700–3300)	N/A	50–100 (160–300)	200–800 (700–2600)	200–600 (700–2000)	20–50 (70–160)
Material feed rate, g/min	30–50	15–50	N/A	150–2000	50–150	25–150	20–50
Deposit/coating							
Density range (%)	85–90	>95	>95	80–95	90–95	90–99	95–99
Bond strength, MPa (ksi:)	7–18 (1–3)	68 (10)	82 (12)	10–40 (1.5–6)	<68 (<10)	>68 (>10)	>68 (>10)
Oxides	High	Moderate to dispersed	Small	Moderate to high	Moderate to coarse	None	None

Figure 1.2: Comparison of thermal spraying processes

Figure 1.2 shows a comparison of thermal spraying process outputs. It is apparent that HVOF provides higher jet temperatures than flame spray, but lower than all other processes. Jet and particle velocities are higher than all other methods save for the detonation gun; its density range is greater than 95% corresponding to very high values, but the process has the

disadvantage of moderate to dispersed oxides which may affect the overall durability of the coating.

Liquid Fuelled HVOF

Liquid-fuelled HVOF guns have gained recent attention due to their generating increased particle momentum and offering improved corrosion resistance (oxidation, gas deposits) over gas systems. They generate a denser coating structure and present better bonding with an increased melting degree control (Kamnis & Gu, 2006) (Tabbara & Gu, 2009) (Basu & Cetegen, 2008); In addition, fuels employed in LHVOF such as kerosene or propane are more economical than their gas counterparts (Kamnis & Gu, 2006). Since the combustion process is heavily influenced by fuel vaporization the design of liquid HVOF gun components has an added degree of complexity; atomization mechanisms must be carefully controlled in order to achieve full combustion. This prevents fuel waste and coating impurities (Tabbara & Gu, 2009).

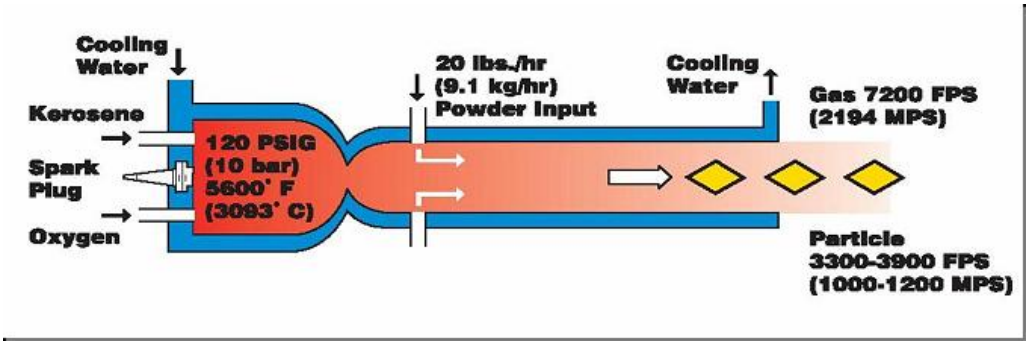

Figure 1.3: Liquid Fuelled HVOF Gun Schematic

1.2 Problem Statement

Although porosities are normal and necessary in thermal barrier coatings, heat treatment and usual service allow hot corrosive gas to reach the coated material, forming thermally grown

oxide (TGO) layers (Jang, Park, Jung, Jang, Choi, & Paik, 2006). Failure of TBCs occurs mostly by cracking, delamination and spalliation of the coating at a TGO layer; this layer is created during heat transfer and while in service, causing eventual crack growth and catastrophic failure. The bond coat plays a very important role in ensuring structural effectiveness and adhesion of the ceramic coating to the coated material. For this reason, there is a necessity to understand and develop increasingly reliable coating techniques.

An inherent problem of the HVOF system is the fact that gas temperatures are much above the melting point of alloys and metals employed in spray powder. Particles may experience oxidation while traveling in the hot gas flow or when impinging on the substrate, resulting in the degradation of the top coat and affecting its overall properties (Katanoda, Morita, Komatsu, & Kuroda, 2011) (Jang, Park, Jung, Jang, Choi, & Paik, 2006). The microstructure of the deposit and its mechanical characteristics are dictated by the velocity, temperature, and oxygen content of particles at the point of impingement. These characteristics are dependent on the physical and chemical state of coating particles upon impact, namely melting degree, velocity and oxidation properties (Tabbara & Gu, 2009) (Li & Christofides, 2005). An understanding of the mechanical and chemical properties, as well as failure mechanisms of the bond coat is essential to improve reliability and lifetime performance of coatings developed by this method (Jang, Park, Jung, Jang, Choi, & Paik, 2006).

1.3 Research Objectives (Global & Local)

HVOF design and modeling involves an intricate interplay between fluid flow, heat transfer, turbulent kinetic energy, completeness of chemical reactions and gas-seeding particle interactions at high temperatures. Since a detailed understanding of the processes mentioned is

essential several design approaches must be made, and combining computational and experimental methods is essential to reach full potential. There are four main processes described in HVOF combustion to be controlled and understood in process optimization for the overall research project (Dongmo, Wenzelburger, & Gadow, 2008):

1- Transformation of chemical energy into thermal energy by fuel combustion in the chamber.
2- Conversion of thermal energy into kinetic energy by expansion through the nozzle and energy transfer from products to particles during this process.
3- Free jet flow field whose patterns depend on the difference between nozzle pressure and atmospheric pressure (defined through under- or over- expansion).
4- Conversion of particle kinetic + thermal energy into work through viscous deformation and surface energy when depositing the coating.

Parameters such as liquid droplet size, injection velocity, location from the substrate and temperature distribution of the HVOF flame and conditions such as temperature and velocity fields all have influence in the final quality and microstructure of a coating (Basu & Cetegen, 2008). While there have been several research projects related to the characterization of HVOF coatings, few works have considered the relationship between extreme environment coating durability and specific gun operating and process limitations, namely O/F ratio, fuel droplet size, combustion chamber pressure and gun geometry. The final aim of the global study is to understand the relationship between these parameters and resulting coating durability for both gaseous and liquid HVOF systems. A thorough understanding of dynamical gas and particle behavior must be obtained through experimental and theoretical processes in order to develop the next-generation HVOF systems.

Global project objectives include studying coating characteristics as a function of operational and process constraints, investigating particle dynamics through particle image velocimetry and varying geometrical parameters to quantify their effect on material properties. The local objectives to be studied in this investigation focus on the development of a liquid-fuelled HVOF gun using a rocket design approach, as well as performing an operability investigation on the developed design. A shear-coaxial injector is used to atomize kerosene droplets; the system is composed of a combustion chamber, converging-diverging nozzle and a barrel section, much like the industrial standard geometry.

1.4 Literature Review

In order to be able to validate any study a review of previous investigations must be performed in order to examine their methods and compare their findings. A short summary of literature related to the subject follows below. It is worth noting that LHVOF combustion has rarely been documented, as few experimental studies have concentrated on these systems. Most research has focused on gas-fuelled systems such as the HV-2000 from Praxair and the Diamond Jet system from Sulzer-Metco (Tabbara & Gu, 2009). A comprehensive understanding of liquid HVOF guns and their interactions with different coating materials can enable the innovation of thermal spraying designs, through meeting the operational requirements of AUSC turbines and boilers.

Past research of HVOF thermal spraying has been mainly focused on computational methods through the simulation of gas and liquid flow in two and three dimensions, using different computational approaches and codes, particularly CFX and FLUENT. Although experimental investigations have been largely performed, they have been mainly focused on the

microstructure of the bond coat as well as in-flight particle diagnosis (Tabbara & Gu, 2009). The combination of computation and physical investigation has seldom been encountered in this subject.

Kamnis (Kamnis & Gu, 2006) provided a 3-D simulation using combustion models available using a finite volume CFD code (FLUENT). They described the flow field and atomization of the fuel, examining velocity, temperature and pressure as a function of distance in the centerline. A droplet diameter distribution for kerosene was obtained through the combustion and discrete particle models; a fixed initial droplet diameter was assumed. The motion of these droplets was coupled with gas flow dynamics in a Lagrangian mode.

An investigation (Tabbara & Gu, 2009) used a commercial CFD code to investigate flow regime and gas flow characteristics, particularly final temperature as a function of radial distance along the centerline. The study is one of the few to combine computational and experimental data. This investigation focused on the JP5000 geometry and changed mesh size to impact both throat diameter and chamber length. The research found a 20% decrease in throat diameter will induce a 60% increase in combustion chamber pressure, increasing downstream velocity as well; a flow of almost perfect condition was described through this geometrical change. A 20% reduction in combustion chamber length yielded realizable results, as there was not an excessive amount of fuel exiting the combustion chamber, and temperature and velocity profiles were not affected significantly. In addition, the study investigated the influence of droplet size on gas flow and flame shape, investigating the complications that accompany using liquid in an HVOF system. The investigation implies that optimization of industrial models is achievable through computational means and that models can be refined; this remains to be tested however as design modifications and their experimental results must accompany such implications. An additional

computational study focused on gas-fuelled systems (Kamali & Binesh, 2009) yielded dependence between axial gas velocity and Mach number on total flow rate and mixture ratio; in this particular study the highest velocity was found to be achieved on the most fuel-rich ratio, corresponding to mixing conditions found in industrial HVOF models.

Katanoda (Katanoda, Morita, Komatsu, & Kuroda, 2011) proposed an experimental procedure to estimate cooling rates for the combustion chamber, mixing chamber and the barrel section of an HVOF gun. A mathematical model was presented to effectively predict pressure and temperature in the mixing chamber for varying rates of fuel, oxygen and nitrogen. Dongmo et. al (Dongmo, Wenzelburger, & Gadow, 2008) investigated and modelled a 3-D gun based on an Eulerian-Lagrangian formulation using the eddy dissipation model, which assumes the reaction rate is limited by the turbulent mixing rate (Dongmo, Wenzelburger, & Gadow, 2008); the study modelled the reaction rate of combustion according to the resultant mass flow of the reactants, namely CO2. Although a different oxidizer/fuel combination (oxygen-propane) is used for this study than for the configuration studied in this paper, temperature and pressure reached 3000 K and 6 bar (Dongmo, Wenzelburger, & Gadow, 2008), similar enough to what is expected in oxygen-methane and oxygen-kerosene combustion. Additionally, the investigation enhanced their results through the modeling of particle injection to discover optimal powder sizing; the study concluded that small particles ($< 20\ \mu m$) are not suitable for this process due to their small mass inertia. Finally, the investigation recommended that fluid-structure coupling and impinging jet influence on the substrate be considered in further modelling approaches.

Li (Li & Christofides, 2005) investigated the former, studying particle melting parameters and substrate forming using a mathematical code; they concluded particles of moderate size achieve higher velocity, temperature and impact than both extremely large and

very small ones. The study found that spray distance has a significant influence on both velocity and melting degree of particles with small sizes; varying this parameter is useful when investigating a new design. Using a mixture of propylene, oxygen and air Li et. al found that Fuel/oxygen ratio plays a very important ratio in particle heating, as flame temperature can be varied through this constraint. An equivalence ratio of 1.2 for this mixture helped to maximize flame temperature and two-phase heat transfer; it is expressed that for industrial applications this is the optimum point for a standoff (distance to substrate) of .2 m under various flow rates. Additionally, they note that a high total gas flow rate helps to maintain gas velocity and temperature in the free jet at optimal levels (Li & Christofides, 2005) for a longer distance leading to better momentum and heat transfer processes between gas and particulates. Generally speaking, the total particle velocity increases as the overall gas flow does, increasing high gas momentum flux in the free jet. Nonetheless, particles do not have to be necessarily fully melted to achieve low coating porosity as long as the deposition efficiency is high. Finally, the study noted that the carrier flow rate must be kept at a minimum to enhance overall transfer of heat, as long as particles can be fed into the flow in the smoothest manner possible.

Basu et al. (Basu & Cetegen, 2008) focused on modeling a thermo physical process in liquid ceramic droplets injected into an HVOF generated jet. The investigation provided a model consisting of several sub-models including aerodynamic droplet break-up, and heat and mass transfer within individual droplets within an HVOF environment. A parametric study was presented according to initial droplet size, concentration of mineral dissolution and the external temperatures and velocities of the HVOF jet to explore processing and injection parameters leading to different morphologies. It was found that the high jet velocity induces shear break-up of the droplets into those of several μm, leading to a better entrainment and heating within the

jet. In this study, the flame at the nozzle exit was characterized by a centerline temperature of about 3000 K and velocities exceeding 800 m/s; in this case, the under expanded supersonic jet became subsonic downstream through a system of oblique shock waves forming a shock diamond pattern.

Few current investigations have analyzed substrate coating features based on equipment design characteristics; those examinations focused on coating properties have done so employing industry-supplied HVOF guns. Physical and mechanical properties of HVOF spray coatings can be analyzed through failure testing such as cyclic loading and performance under high temperature conditions (Jang, Park, Jung, Jang, Choi, & Paik, 2006). Final coating characteristics may also be analyzed in a scanning electron microscope (Bach, Mohwald, Engl, Drobler, & Hartz, 2006) for detailed visuals on porosity and composition. One example of such study is that of Jang et. al (Jang, Park, Jung, Jang, Choi, & Paik, 2006), who researched Co-Ni alloy coatings on a nickel-based superalloy substrate. In this investigation mechanical properties such as hardness H and modulus E were studied as a function of the thickness of the bond coat, as these values are essential in improving reliability and lifetime performance for thermal environments. In their results, the interface between the HVOF applied bond coat and substrate showed a relatively continuous microstructure, with the bond coat appreciated to be quite dense (Jang, Park, Jung, Jang, Choi, & Paik, 2006); on the other hand, those samples prepared by the atomic plasma spray (APS) process showed slight cracking. Additionally, the thermally grown oxide (TGO) layer formed during fatigue tests tended to increase as a function of temperature and dwell time, but was found to be independent of applied bond coat thickness.

Chapter 2: HVOF Design

The modeling of HVOF systems is considered to be quite intricate, due to the fact that the overall process combines combustion and heat transfer processes, along with compressible supersonic flow, high-turbulence mixing and multiphase interactions if the fuel is liquid (Tabbara & Gu, 2009).The physical and mechanical characteristics of HVOF coatings are influenced by the microstructure of the coating, which itself is a function of the chemical state of particles at their point of impact (namely velocity, temperature, melting degree and content of oxides) (Dongmo, Wenzelburger, & Gadow, 2008). The mentioned variables are dependent on process parameters of the gun such as O/F ratio, nozzle cross sectional area, deposit spraying distance and powder density distribution.

The optimization of HVOF guns relies on costly trial and error procedures; although cost-intensive, it is a reliable method to investigate HVOF processes (Dongmo, Wenzelburger, & Gadow, 2008). In the industrial HVOF process environment it is important to be able to control particle velocity and melting degree in order to achieve desired coating properties; a manipulation of these parameters can be achieved by adjusting gas momentum flux and overall temperature (Li & Christofides, 2005). Designing and modelling a spray gun effectively is critical to achieve consistency and superior performance from the generated coatings.

The basic features incorporated into an internal combustion HVOF are defined to be the water cooling system, particle injection method and nozzle geometry (Davis, 2004); they must be refined, tested and improved accordingly to enhance coating characteristics. Careful consideration has been given to each of these individual features in order to replicate the conditions of an industrial HVOF gun.

Following is a summary of the design approach handled to develop a kerosene-fuelled HVOF gun. Steady state combustion in a rocket design includes injection, atomization, vaporization, mixing with oxidizer and combustion (Kamnis & Gu, 2006). The process is started through the injection and vaporization of the liquid component; this mechanism defines the flow field and combustion characteristics inside the combustion chamber. The overall setup consists of an injector, combustion chamber, converging/diverging nozzle and a barrel section. Although the equations for the setup presented below, save for the injector parameters, are designed for a gas-gas configuration, a liquid-gas approach should work as true too once atomization and vaporization of the fuel has been performed.

2.1 Initial Design Parameters

Initial limitations must be chosen in order to serve as constants from which geometrical constraints will emerge. Though industrial parameters dictate the throat diameter to be approximately 7 mm, this value was deemed as 15 mm due to machinability issues in the project. As long as the outputs match or exceed literature reference values geometry can be seen as a changing parameter. Desired combustion pressure and temperature are predefined as 7 bar and 3350 K; this is due to the fact that HVOF guns employing kerosene-oxygen combustion present a pressure between 5-10 bar, while combustion chamber temperatures range around 3000 K (Katanoda, Morita, Komatsu, & Kuroda, 2011). The book “modern engineering for design of liquid-propellant rocket engines” (Huzel & Huang, 1992) serves as a general guide in terms of equations, reference values and graphs. Specific heat ratio is assumed to be 1.2 as this is the general value for hydrocarbon-oxidizer mixtures; the oxidizer-fuel ratio is set as slightly rich, as most industrial configurations operate in this manner. A summary of the initial parameters chosen for this LHVOF configuration can be seen in the table below.

Table 2.1: Initial Design Conditions

Symbol	Name	Value	Units
D_t	Throat Diameter	15	mm
P_c	Chamber Pressure	7	bar
γ	Specific Heat ratio	--	--
g	Gravitational acceleration	9.81	m/s^2
$\bar{R}$	Adapted Universal Gas Constant	--	--
M_{wt}	Molecular Weight of Gases	--	--
T_c	Combustion Chamber Temperature	3350	K
O/F	Oxygen to Fuel Ratio	--	--

Throat area is to be obtained assuming a circular cross-section; total mass flow rate of the gases is a function of several initial parameters and can be calculated assuming ideal gas law theory (Huzel & Huang, 1992). The oxidizer and fuel combination mass flow rates can be calculated according to the desired O/F ratio. It is worth noting that although total mass flow rate may remain the same, flame structure, temperature and shape are dependent on this ratio. Additionally, injector geometry is a function of the required individual flow; for this reason a range of mixing ratios must be determined beforehand to ensure optimal mixing. The equations used to calculate oxidizer and fuel flow rates follow below; Table 2.2 shows their final values in two unit systems.

$$A_t = \frac{\pi D_t^2}{4} \tag{1}$$

$$\dot{m_t} = .318 * A_t * P_c * \sqrt{\frac{\gamma * g}{R * T_c} * \left[\frac{2}{\gamma + 1}\right]^{\frac{\gamma+1}{\gamma-1}}} \tag{2}$$

$$\dot{m_t} = \dot{m_o} + \dot{m_f} \tag{3}$$

$$\dot{m_o} = \frac{\dot{m_t} * {}^{O}/_{F}}{({}^{O}/_{F} + 1)} \tag{4}$$

$$\dot{m_f} = \frac{\dot{m_t}}{({}^{O}/_{F} + 1)} \tag{5}$$

Table 2.2 General Design Results

Symbol	Name	Value	Units
A_t	Throat Area	176.13	mm^2
R	Gas Constant	--	--
$\dot{m}_t$	Total Gas Flow Rate	.085	kg/s
$\dot{m}_o$	Oxygen Mass Flow Rate	.064	kg/s
$\dot{m}_f$	Fuel Mass Flow Rate	.021	kg/s

2.2 Injector

An adequate injector should fulfill basic needs for operational use, depending particularly upon its configuration (liquid-gas, gas-gas etc.). It must ensure a quick rate of evaporation through the atomization of the liquid component, enable rapid and full mixing of the fuel and

oxidizer, and deliver the gases at a sufficiently high rate with a high enough pressure in the line so that flashback is avoided and no significant pressure variations occur. (Sutton & Biblarz, 2010) (Sutton G. , 2005) (Yang, Habiballah, Popp, & Hulka, 2005)

Injector quality is determined by performing cold flow tests using inert liquids with similar properties as the gases. Water is usually employed to confirm pressure drops at different flows; the simulation fluid should be approximately of the same density and viscosity as the required components (Sutton & Biblarz, 2010). All new injectors are hot fired and tested with actual mixtures before continuous use. Fuel/oxidizer atomization, combustion and mixing characteristics cannot be analyzed until a hot-firing session is performed. Subsequent designs are highly influenced by experimental data of the first prototype. For a given combination, chemical reactions and kinetics of stream breakup, mixing, droplet formation and heat transfer must be studied and fully understood before an approach is established (Ibrahim, Kenny, & Walker, 2010) (Salgues, Mouis, Lee, Kalitan, Pal, & Santoro, 2006).

A shear-coaxial injector was chosen for this formation, due to the multiphase characteristics of the flow. In this configuration gaseous oxidizer flows through a central post (most shear coaxial injectors employ a liquid oxidizer and gaseous fuel, making the central post liquid (Huzel & Huang, 1992); kerosene flows coaxially in an outer ring. The differential velocity causes a shear between the fluids helping to atomize the slower stream (Sutton & Biblarz, 2010). Before injection is completed oxidizer and fuel begin to mix and create turbulence through a recess space. The interactions between liquid and gaseous environment create instabilities, dissolving the liquid stream into small droplets, which disperse and evaporate (Ibrahim, Kenny, & Walker, 2010). The overall objective for this HVOF configuration is to be able to allow for both gas-gas and gas-liquid operations. Since gaseous mixing is not as

complicated a process as multiphase interactions the injector must be suitable for both arrangements with adjustments in overall flow rates to reach similar points. Combustion phenomena are highly affected by the number of injection ports (Metjet employs three ports while Praxair's JP5000 has only one). For this arrangement three ports have been chosen; future injector designs will vary this number to fully understand the impact in mixing and atomization. The planned and built injector configuration can be seen in Figure 2.1. Although only a cutout of the design is seen, it can be perceived that liquid flows around the oxidizer post in a series of small passages before completely mixing and entering the chamber. The overall fuel line is divided into two small separate segments in the setup; the main passage mixes with the oxidizer and constitutes most of the fuel flow. The small, separate line is designed for film cooling use.

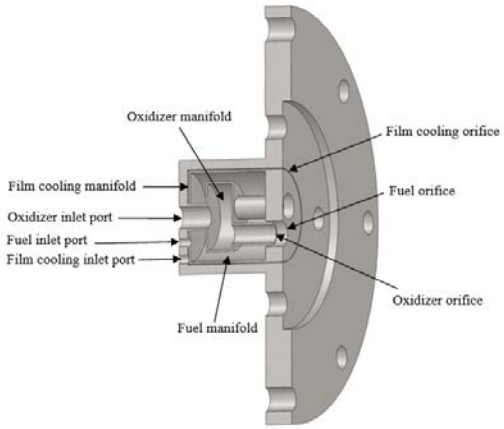

Figure 2.4: Injector schematic

Film cooling is a method applied to chambers and nozzles, where a relatively cool film protects wall surfaces from excessive heat transfer (Sutton & Biblarz, 2010). Extra fuel can be used through injection holes near the outer layers of the injector, to be vaporized completely before the throat. Film cooling is usually required in LHVOF guns due to their high combustion temperatures as it protects the chamber wall with a thin film of unburned fuel, lowering the mixture ratio of any errant streaks in the flow.

Pressure drop in industry standard HVOF gun varies from 10 to 25 percent of overall chamber pressures. In rocket engines, an initial pressure drop of 20% is recommended to avoid pressure instabilities affecting the setup. A combustion pressure variation of only 5% has been found to have a significant impact on the overall behavior and efficiency of a system (Huzel & Huang, 1992). A low pressure drop is usually desirable when overall weight of the injection system must be minimized, but high pressure drops reduce or eliminate combustion instability and increase liquid atomization (Sutton & Biblarz, 2010). Initial injector pressure drops have been assumed according to the desired line pressurization as well as their inner diameter. A 15% pressure drop is assumed for the kerosene line; a 40% pressure drop has been set for the oxidizer line.

The discharge coefficient influences final velocities according to a given pressure drop in an injector. This value is at a maximum when the discharge coefficient is one. Smooth and well-rounded entrances to the injection holes result in large values of the constant. For a short-tube with a rounded entrance the discharge coefficient varies between .7 and .9 depending on exit diameter (Sutton & Biblarz, 2010); ultimately the discharge coefficient is a function of orifice geometry (generally classified as sharp edged, rounded, conical, or spiral). Initial injector design values follow in Table 2.3. As previously mentioned, injector design is a function of the mass flow rates of the oxidizer and fuel.

Table 2.3: Initial Injector Values

Symbol	**Name**	**Value**	**Units**
N	Number of orifices	3	--
C_d	Dimensionless Discharge	.75	--

ΔP_f	Injector Pressure Drop in Fuel Line	105000	Pa
ΔP_o	Injector Pressure Drop in Oxidizer Line	275000	Pa
ρ_f	Fuel Density (Kerosene)	807	Kg/m^3
$\rho_{o@atm}$	Oxidizer Density	1.33	Kg/m^3
t_o	Thickness of Oxidizer Post	1	mm

Injector pressure is determined as a function of desired pressure drop and combustion pressure for both lines. Pressure measurement devices could in theory be placed in the line at the point previous to injection and in the combustion chamber to ensure the accuracy of the drop measurement. Equations 6 and 7 are included for the case of compressible flows both in the oxidizer as well as in the fuel. In the case of kerosene this value is maintained for the following calculations due to its liquid properties. The individual areas for the fuel and oxidizer can be calculated according to the desired number of ports, mass flow rate and pressure drop values. Equations 6-14 describe this method and Table 2.4 exhibits the results. Since a coaxial type injector includes an annulus fuel diameters are chosen according to the oxidizer calculation as well as the desired thickness of the post; oxidizer and fuel orifice diameters are rounded to the next available mm due to possible machinability issues.

$$P_o = P_c + \Delta P_o \tag{6}$$

$$P_f = P_c + \Delta P_f \tag{7}$$

$$\rho_o = \frac{P_o * \rho_{o@atm}}{P_{atm}} \tag{8}$$

$$\rho_f = \frac{P_f * \rho_{f@atm}}{P_{atm}} \tag{9}$$

$$A_o = \frac{\dot{m_o}}{N * C_d * \sqrt{2 * g * \rho_o * \Delta P_o}} \tag{10}$$

$$A_f = \frac{\dot{m_f}}{N * C_d * \sqrt{2 * g * \rho_f * \Delta P_f}} \tag{11}$$

$$D_{oi} = \sqrt{\frac{4A_o}{\pi}} \tag{12}$$

$$D_{oo} = D_{oi} + t_o \tag{13}$$

$$D_f = \sqrt{\frac{4A_f}{\pi} + {D_{oo}}^2} \tag{14}$$

Table 2.4: Resultant Injector Parameters

Symbol	Name	Value	Units
P_f	Fuel Line Pressure	805000	Pa
P_o	Oxidizer Line Pressure	975000	Pa
D_{oi}	Oxidizer Orifice Inner Diameter	3	mm
D_{oo}	Oxidizer Orifice Outer Diameter	5	mm
D_f	Fuel Orifice Diameter	6	mm

Following is the schematic for a single port according to the calculated measurements. The recess distance has been set as 5 mm to ensure proper mixing before entering the combustion chamber. Overall diameter for a single port is 6 mm. Recess wall thickness has been set to be 1mm due to machinability limits, as well as to ensure a sturdy design capable of withstanding pressure variations.

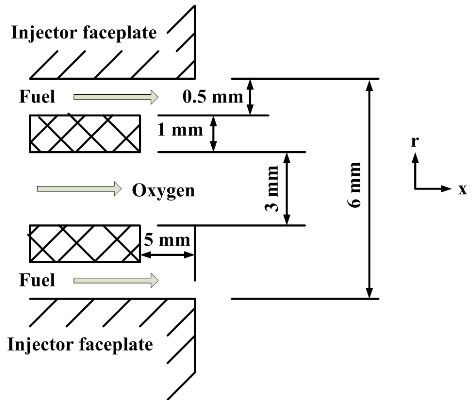

Figure 2.5: Designed Injector Geometry

2.3 Combustion Chamber

The combustion chamber is the part of a cavity where mixing and burning of the gases takes place. Since combustion temperature is always higher than the melting point of the materials that compose it, a cooling system is usually required for its safe operation (Sutton & Biblarz, 2010). If a cooling structure is not included, a monitoring system can be employed to stop combustion before a critical point is reached. The general geometry of a combustion chamber with accompanying geometry is seen in the figure below.

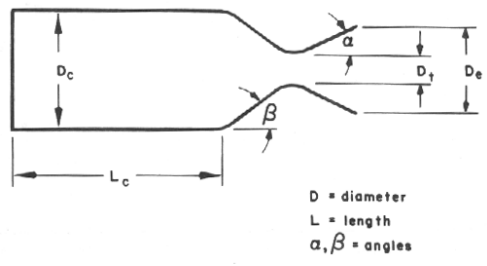

Figure 2.6: Combustion Chamber Schematic

Chamber volume is defined as that volume up to the end of the converging section. The total volume must be large enough to ensure mixing, evaporation and complete combustion (Sutton & Biblarz, 2010). A chamber that is too small will produce incomplete combustion and inadequate performance. In order to reduce losses attributable to flow velocity the combustion chamber area should be at least three times the nozzle throat area $\left(\frac{A_c}{A_t} \geq 3\right)$ (Yang, Habiballah, Popp, & Hulka, 2005). Additionally, in small combustion chambers the diameter dimensions should be three to five times that of the nozzle in order to have maximum usability by the injector configuration (Sutton & Biblarz, 2010) (Yang, Habiballah, Popp, & Hulka, 2005). Due to the nozzle throat diameter having been chosen as 15 mm, chamber diameter has been set to an initial value of 50 mm, corresponding to 3.33 times the former value in diameter and 11 times the throat area. Using the nozzle area concept outlined above the minimum value for this diameter is calculated to be 26.5 mm.

A parameter describing chamber volume required for complete combustion is defined as the characteristic chamber length (equation 16); it is essentially a substitute for determining chamber residence of the oxidizer and fuel mixture. Characteristic length converts overall combustion chamber volume, equating it into that of a straight tube. The determination of wall thickness outlined by equation 17 is a function of chamber geometry, material properties and desired maximum pressure. While a safety factor is included in the calculation and will directly

proportionately increase the value of chamber thickness the cooling system must be taken into account; a compromise between strength and heat conductive properties must be achieved. Inputs and outputs for the configuration are outlined in the tables shown below; the formulas used for these calculations correspond to equations 15-17.

Table 2.5: Combustion Chamber Parameters

Symbol	Name	Value	Units
β	Converging half-angle	20	Degrees
A_t	Throat Area	.000176	m^2
L_c	Combustion chamber length	.11	m
--	Safety factor	3	--
P_c	Combustion chamber pressure	700000	Pa
D_c	Combustion chamber diameter	.05	m
A_c	Combustion chamber area	.00196	m^2
S	Allowable working stress of camber material	10000000	Pa

$$V_c = A_t \left[\frac{L_c * A_c}{A_t} + \frac{1}{3}\sqrt{\frac{A_t}{\pi}} * Cot\ \beta \left(\left(\frac{A_c}{A_t}\right)^{\frac{1}{3}} - 1 \right) \right] \quad (15)$$

$$L^* = \frac{V_c}{A_t} \quad (16)$$

$$t_w = \frac{P_c * D_c}{2 * S} * \text{safety factor} \quad (17)$$

Table 2.6: Combustion Chamber Calculated Geometry

Symbol	Name	Value	Units
V_c	Combustion chamber volume	$1.5*10^{-4}$	m^3
L^*	Characteristic chamber length	.85	m
t_w	Chamber wall thickness	.005	m

2.4 Converging Diverging Nozzle

A converging diverging nozzle, also called a De Laval nozzle, allows thermal energy generated in the combustion process to convert to kinetic energy through the compression of the gas. As seen in the figure below a high pressure, low velocity flow is converted to a high-velocity low pressure gas through the change in flow cross sectional area. In rockets, since thrust is the production of mass flow rate and gas velocity, a high kinetic energy is desirable. In HVOF guns, high momentum is also desirable, due to the fact that particles must have a high velocity when impinging on a substrate.

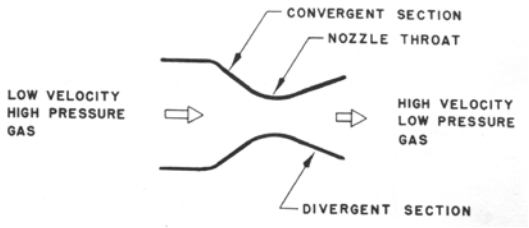

Figure 2.7: Converging-Diverging Nozzle Process

As long as a sufficiently large nozzle pressure ratio (NPR) is maintained, gas will accelerate up to sonic velocity at the throat and achieve a supersonic rating in the divergent section of the design. The static nozzle pressure at the throat P_t is defined as the critical pressure (Sutton & Biblarz, 2010). De Laval nozzles have the characteristic of sonic throat velocity being

maintained even when exit or ambient pressure conditions are greater; in order to maintain this condition pressure adjustments in the form of subsonic deceleration or shock waves (usually present in HVOF systems). Throat pressure and temperature can be calculated through equations 18 and 19; these values will always be lesser than those generated in the combustion chamber due to the energy conversion through gas acceleration (Sutton & Biblarz, 2010). A converging angle of 20 degrees and a diverging angle of 15 degrees have been chosen due to these values having been standardized in rocket design (Huzel & Huang, 1992). Nozzle exit conditions such as Mach number, total area and temperature are outlined in the equations and tables below. Exit area defines the barrel section cross-sectional geometry.

Table 2.7: Converging-Diverging Nozzle Conditions

Symbol	Name	Value	Units
β	Converging half-angle	20	Degrees
α	Diverging half-angle	15	Degrees
T_c	Combustion chamber temperature	3350	K
γ	Specific heat ratio	1.2	--
P_c	Combustion chamber pressure	700000	Pa
P_{atm}	Atmospheric pressure	101300	Pa

$$T_t = T_c \left[\frac{1}{1 + \frac{\gamma - 1}{2}} \right] \tag{18}$$

$$\mathrm{P_t} = \mathrm{P_c}\left[1 + \frac{\gamma - 1}{2}\right]^{\frac{-\gamma}{\gamma-1}} \tag{19}$$

$$\mathrm{M_{a_e}} = \sqrt{\frac{2}{\gamma - 1}\left[\left(\frac{\mathrm{P_c}}{\mathrm{P_{atm}}}\right)^{\frac{\gamma-1}{\gamma}} - 1\right]} \tag{20}$$

$$V_e = \sqrt{\frac{2 * g * \gamma * R * T_c}{\gamma - 1}\left[1 - \left(\frac{P_{atm}}{P_c}\right)^{\frac{\gamma-1}{\gamma}}\right]} \tag{21}$$

$$T_e = T_t\left(\frac{P_{atm}}{P_t}\right)^{\frac{\gamma-1}{\gamma}} \tag{22}$$

$$\mathrm{A_e} = \frac{\mathrm{A_t}}{\mathrm{M_{a_e}}}\left[\frac{1 + \frac{\gamma - 1}{2}\mathrm{M_{a_e}^2}}{\frac{\gamma + 1}{2}}\right]^{\frac{\gamma+1}{2(\gamma-1)}} \tag{23}$$

$$D_e = \sqrt{\pi\frac{A_e}{4}} \tag{24}$$

$$NPR = \frac{\mathrm{P_t}}{\mathrm{P_c}} \tag{25}$$

Table 2.8: Exit Values for Nozzle

Symbol	Name	Value	Units
T_t	Throat Temperature	3045	K
P_t	Throat Pressure	395000	Pa
M_{a_e}	Exit Mach Number	1.9	--
V_e	Exit Velocity	1690	m/s
T_e	Exit Temperature	2475	K
D_e	Exit Diameter	.021	m
NPR	Nozzle Pressure Ratio	.56	--

2.5 Barrel Section

Powder particles can either be fed through the oxidizer stream or at some location downstream. The former has several disadvantages including and not limited to particle overheating, wrongful deposition and deposition inside the configuration; nevertheless, it also solves the question on how to effectively introduce seeding powder into a HVOF system.

In order to decrease the possibility of overheating and introduce particles directly to supersonic flow (Katanoda, Morita, Komatsu, & Kuroda, 2011) most gun configurations inject particles into the barrel through a tapping angle. Computational investigations such as that by Kamali (Kamali & Binesh, 2009) also make this assumption. The barrel has been designed as the section where particle injection occurs and products exit the configuration. Barrel geometry in HVOF systems is said to vary between 8 and 30 cm (Davis, 2004). Barrel length in this design

has been established to be 10 cm in order to have sufficient spacing for particle integration into the flow; an optimization of barrel lengths can be performed through experimental means.

2.6 Cooling System

Heat is transferred to all surfaces exposed to hot gases, namely the injector faceplate, chamber, nozzle and barrel section walls. A typical heat transfer rate distribution identifies the highest temperature at the nozzle of the rocket, with quickly decreasing values as the exit approaches. The largest part of the heat is transferred by means of convection (Sutton & Biblarz, 2010). Usually 5 to 35 % of heat transferred to the walls can be attributed to radiation.

Extremely high temperatures can cause the chamber or nozzle to fail, as most materials become weaker when exposed to thermal stresses. A steady state cooling has been chosen as opposed to a transient heat transfer method in order to avoid miscalculations and diminishing the possibility of extreme well temperatures. In transient heat transfer the heat absorbing capacity of the material determines the duration of the firing (in these systems combustion is stopped just before failure).

A cooling system effectively prevents the melting of the combustion chamber, nozzle and barrel section. The designed cooling environment for this system consists of a cylinder surrounding all external faces of the HVOF gun. This geometry forms a passage where coolant enters the system through the top and exits through the bottom. Coolant is pushed through the structure using a pump and cooled before recirculation employing a heat exchanger. Though water and air are the most common coolants employed in HVOF systems an alternate fluid has been considered for the project. Dynalene is a variation of ethylene glycol with superior heat absorbing qualities; some of its properties are outlined in the table below.

Table 2.9: Properties of Dynalene *(Dynalene Company)*

Properties	**Dynalene (HC-10)**
Temperature range (℃)	-10 to 218
Specific Heat capacity, (KJ/Kg.K)	3.28
Density (Kg/m^3)	1200

The theoretical heat transfer from the setup to the cooling system can be calculated by equation 27 through the postulation that the area of the nozzle converging cone is 10% of the total chamber area. The total mass flow rate for Dynalene is to be calculated through the desired values for inlet and exit temperatures of the fluid. Outflowing temperature should never be assumed to be greater than the vaporization temperature of the coolant. Flow passage geometry can be obtained through the assumption of a minimum flow velocity inside the chamber as well as defining cross sectional geometry as an annular passage where the inner diameter is the outer surface of the gun.

Table 2.10: Required Cooling Values

Symbol	**Name**	**Value**	**Units**
D_c	Combustion Chamber Diameter	.05	m
t_w	Chamber Wall Thickness	.005	m
L_{barrel}	Barrel Section Length	.1	m
D_{barrel}	Barrel Section Diameter	.021	m
L_c	Combustion Chamber Length	.11	m
q	Average HVOF heat transfer rate	6	MW/m^2
$C_{p_{coolant}}$	Coolant heat capacity	3.28	KJ/Kg.K

$$A_{total} \cong 1.1 * \pi * L_c(D_c + 2 * t_w) + \pi * L_{barrel}(D_{barrel} + 2 * t_w) \quad (26)$$

$$Q_{total} = q * A_{total} \quad (27)$$

$$\dot{m}_{coolant} = \frac{Q_{total}}{C_{p_{coolant}} * (T_o - T_i)_{coolant}} \quad (28)$$

$$A_{cooling\ jacket} = \frac{\dot{m}_{coolant}}{\rho_{coolant} * V_{coolant}} \quad (29)$$

$$A_{cooling\ jacket} = \frac{\pi}{4}\left(D_o^2 - D_i^2\right) \quad (30)$$

$$D_i = D_c + 2 * t_w \quad (31)$$

Table 2.11: Cooling Resultant Values

Symbol	Name	Value	Units
A_{total}	Setup Area to be cooled	.0325	m^2
Q_{total}	Total Heat Transferred	.195	MW
D_i	Theoretical cooling jacket inner diameter	.085	m
D_c	Theoretical cooling jacket outer diameter	.1	m

Chapter 3: Methodology

3.1 Test Rig

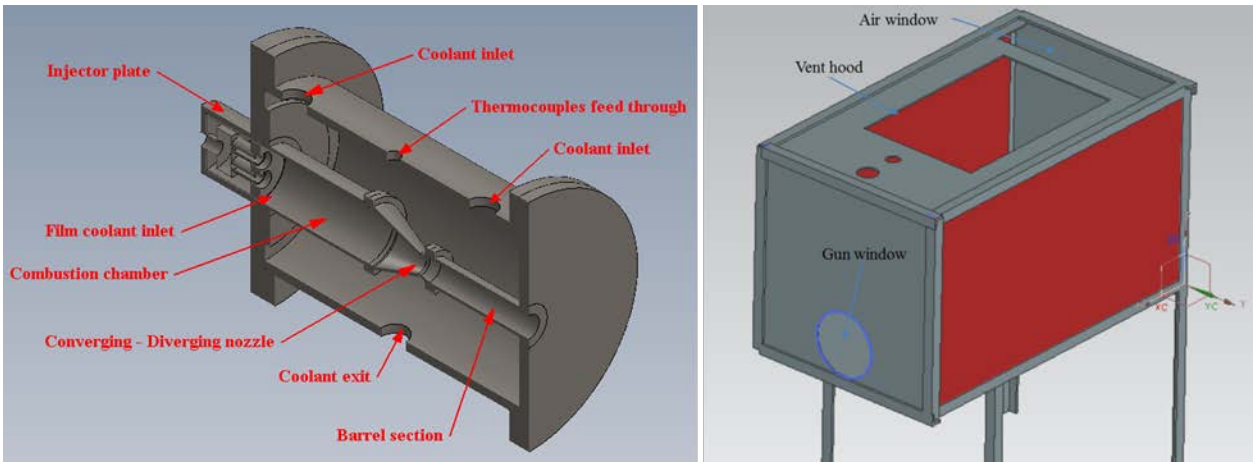

Figure 3.8: General Setup Schematic and Exhaust Enclosure

A final schematic of the final design of the HVOF gun is seen in Figure 3.1. The combustion chamber has been laser-welded to the converging section; the barrel section has been welded to the divergent segment. The design of this setup allows for easy removal and cleaning of the main components through flanges on both sides of the cooling chamber. The injector is independently welded to a flange which attaches to the combustion chamber. This was considered as such to ensure proper sealing and no coolant leaks reaching the inside of the configuration. Initial line formation and testing plan employs a gaseous fuel (methane) for setup behavior examination and added safety considerations. Kerosene is to be used once gas-gas combustion has been thoroughly investigated in the system. A venting enclosure (Figure 3.2) has been built as a confining volume to prevent plume expansion and possible damage to nearby laboratory instrumentation. All walls save the lateral geometries are composed of stainless steel. Lateral walls are covered in fire proof blankets rated up to 1500 K in short term exposure

(Pyroblanket 32oz). Recently, two internal deflectors were added to the design as to prevent damage to vent hood equipment. A stainless steel kitchen range hood has been added to the top of this enclosure to properly draw out combustion products into the laboratory main suction vent. The combustion process is seen orthogonally through the left side of the setup exit; at this location a small piece of the fire blanket has been lifted to allow for sufficient viewing space. The schematic of the design can be viewed as compared to machined product in the schematic below.

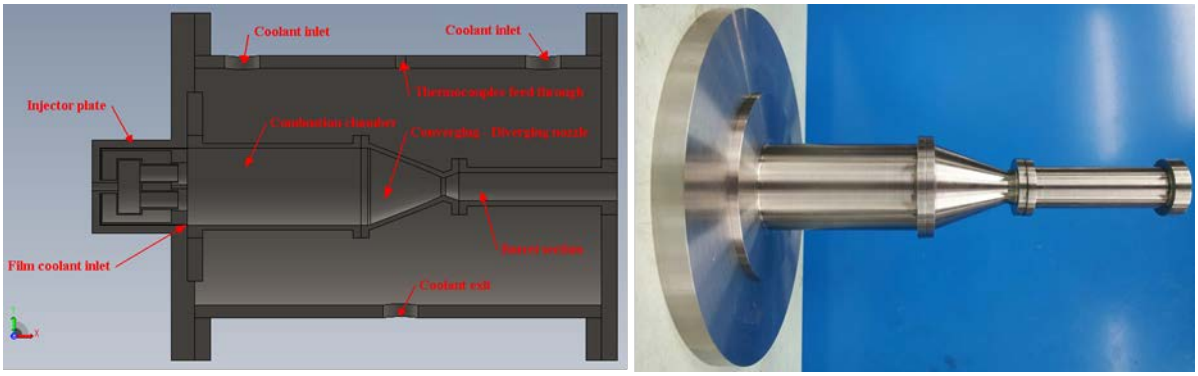

Figure 3.9: Designed vs. machined HVOF gun *(Mohamed, Cabrera, Love, & Choudhuri, 2014)*

The test rig consists of five lines: oxidizer, fuel, purging, external torch and cooling, each one consisting of a combination of measuring and safety devices. The overall setup including all components can be seen in Figure 3.3. The cooling line begins with a 100 gallon storage tank, followed by a shutoff valve and a 1.5 HP centrifugal pump to circulate the fluid on the 1" line. A liquid turbine flowmeter is used in the line before injection into the cooling chamber to ensure sufficient flow for heat exchange. After exiting the gun configuration the flow runs through an analog thermometer and enters a heat exchanger equipped with 8 axial fans. The heat exchanger output is delivered back to the storage tank.

The oxidizer line begins with one, two, or three oxidizer tanks, dependent upon the required volumetric flow. A solenoid valve follows for remote and accurate ON/OFF control of the flow; a pressure relief valve is placed after this to prevent excessive pressure buildup in the line. At this point a gas flow meter (1000 SLPM) monitors and transmits the flow information to the PC. Accuracy of the flowmeter in high flow rates (above 200 SLPM) has been set to be +/- 1.5% of full scale, or 15 SLPM. A check valve is placed in the line to avoid flow reversal, and a pressure transducer (accuracy +/- 1.25 psig) monitors final line pressure before injection. Oxidizer line diameter is ¾".

The fuel line (CH4) begins with a single tank, followed by a solenoid valve. A pressure relief valve is implemented in the sequence, much like in the oxygen line. An Omega gas flowmeter (500 SLPM) measures and reports this value for storage; in the case of high flows an accuracy of 1% or +/- 5 SLPM is acceptable. After a check valve, a transducer analyzes line pressurization before injection is attempted (accuracy +/-1.25 psig). Fuel line diameter is ½". The external torch line employs only a solenoid valve for ON/OFF operation, a flow meter (to ensure flow is within range) and a check valve to prevent reversed flow and/or flashback. Finally, the purging line begins with a solenoid valve to make automation possible, followed by a line divergence, each section going into a gas protected by a check valve to prevent mixing. Purging times may vary according to overall gas flow rate, but a baseline minimum measurement for gas evacuation has been determined to be 5 seconds at a nitrogen tank pressure of 100 psi.

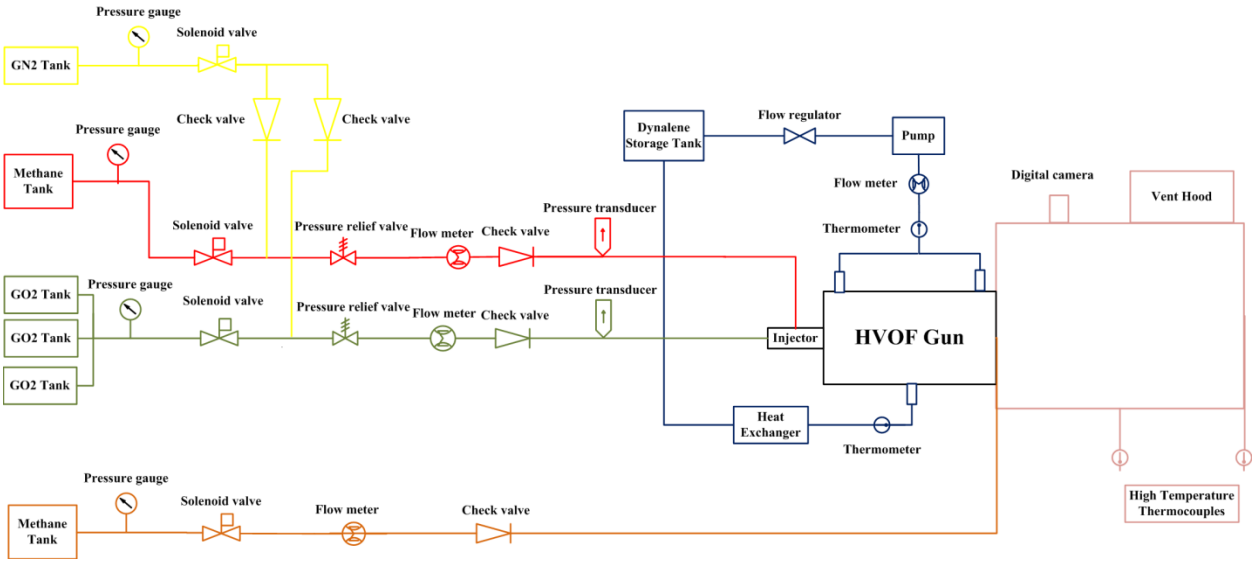

Figure 3.10: General Line Schematic

The igniter configuration is equipped with a single sided copper lead ignition system powered by 25K VDC generated by a voltage transformer. Voltage input is 12 VDC with variable current generated by a quad output DC power supply. A simple schematic of all electronic lines is shown in Figure 3.4. The data acquisition system (DAQ) provides an output in the form of a duty cycle to activate fan rotation frequency for the cooling line; the DAQ also provides a signal to the solenoid valves through a relay, which in turn indicates their ON/OFF sequence. The DAQ receives data from the flow meters and pressure transducers in the form of voltage and converts it to an actual reading; since the output of the PTs is measured in mV, programmable voltage converters must always be included in the wiring setup. Low and high temperature thermocouple data is also received and interpreted by the DAQ. The cooling pump and heat exchanger fans are wired to the laboratory grid in terms of power supplement. The separate DC power supply provides voltage and current to the transformer box for the igniter as well as to all employed solenoid valves. An emergency stop button is hard-wired in all supplied configurations to prevent further combustion in case of an emergency.

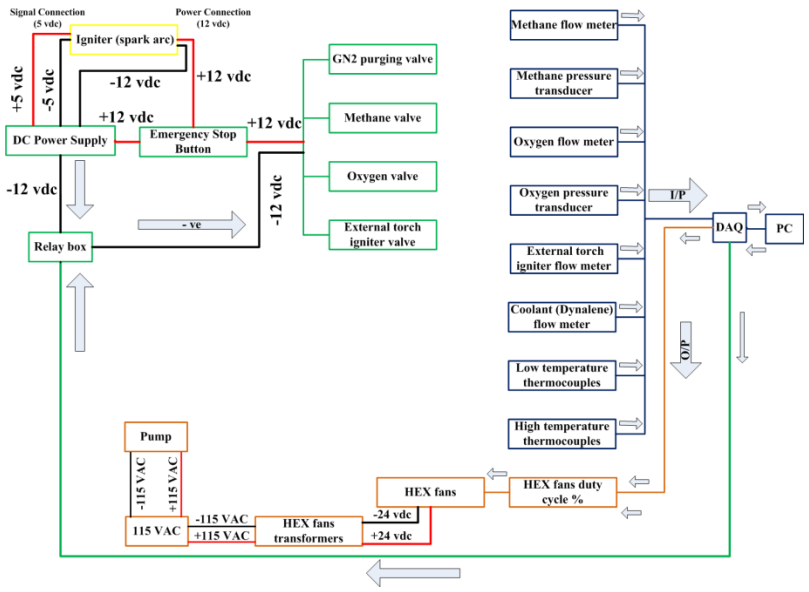

Figure 3.11: Electrical Device Diagram

Figure 3.5 shows the general interface for the generated LabView program. A monitoring of coolant, oxidizer and fuel flows is essential for all combustion testing; the powder flow measurement is required only when coating is the main goal of the session. Oxidizer, fuel and powder pressure monitoring is essential to relate flow measurements to a standard line condition, as the primary parameter for all lines is tank pressurization. Flows are to be determined as a function of this initial condition to ensure repeatability. A monitoring of temperatures through thermocouples guarantees cooling rate is sufficient for the gun setup and provides an estimation of temperature for outside jet conditions.

Due to the characteristics of the fans a duty cycle must be established to exhibit a response in terms of RPM. Initial movement occurs at around 40% of duty cycle, with a proportional increment in radial velocity. Note that the outside torch is not included in this interface; it is assumed that when producing coatings an adequate ignition control is present to prevent substrate overheating. All three solenoid valves are controlled remotely though ON/OFF switches. Ignition is remotely controlled by a similar switch; it remains to be added to the

particular interface shown. Setup may be controlled either manually or automatically; a sequence of valve opening and closing times must be previously determined for the latter mode.

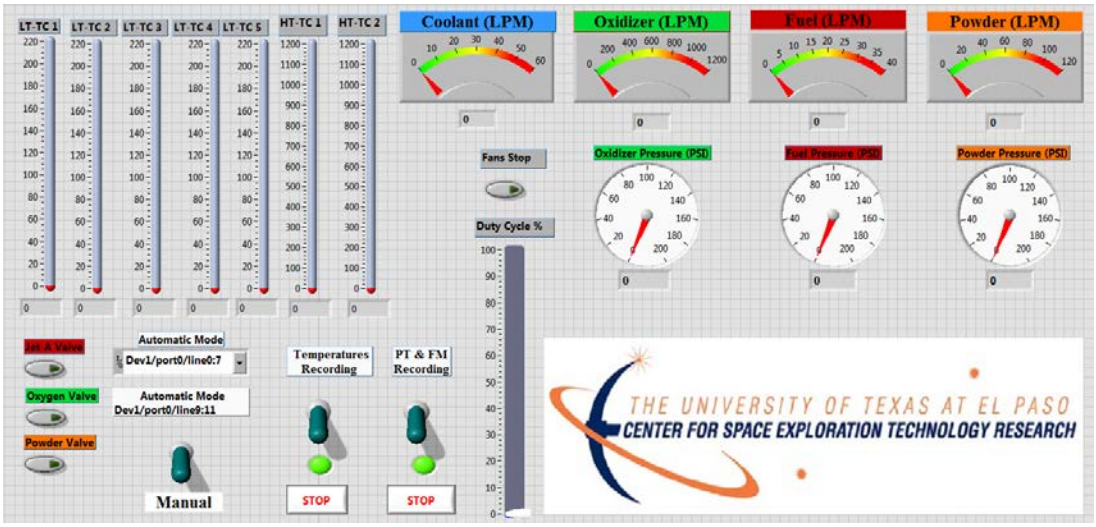

Figure 3.12: Labview Interface

3.2 Safety Considerations

A fast-acting, automatic control of solenoid valves is essential in the event of an emergency. Emergency switches must be present both in the interface as well as in a physical location; this is due to the possibility of software malfunction during a test, which could cause significant damage to the setup components. A manual button has been implemented in the operation control center, and it is readily available. At least one person during a test must take control of the switch in order to halt combustion at will. A fire extinguisher is to be on-hand at all times in the event of an uncontrolled firing. Off-setup, undesired combustion must be continuously prevented; an unburned hydrocarbon-monitoring device must be used before, after and in-between runs. In the case of setup malfunctioning or overpressure, explosion-proof Kevlar walls are placed around the experimental area to protect all operators present. To prevent these

events, continuous purging of the lines has been implemented into the test procedure; additionally, wait times have been established for venting possibly hazardous gases.

To reduce the possibility of an unplanned fire the nozzle must be examined and cleaned in between runs; examination of the device is conducted using a boroscope or small, maneuverable camera. Although most experimentation is performed under a manual mode, redlines must be established in automatic operation. Redlines are defined as overall safety limits; once the system detects a breaching of established boundaries, all operations must be halted. An oxygen monitor is employed to detect abnormal levels in the atmosphere; if a leak exists for inert gases or an enriched oxygen atmosphere is detected a signal will be transmitted. Due to the fact that noise levels for HVOF systems can range anywhere from 125 to 133 dba (Davis, 2004), all those present are required to wear adequate ear protection. As a final note on safety, no one except test operators is allowed to be in the laboratory during a session.

3.3 Roles

Specific roles are assigned according to the number of operations required for a particular test. Basic roles included in experimental procedure and their responsibilities are as follows:

- Hardware Technician: Responsible for monitoring tank pressure, inspecting all hardware components, operating external torch systems and running cooling and ventilation subsystems.
- Test Conductor: In charge of operating LabView interface, informing hardware technician of adequate tank pressures and operating emergency procedure.
- Test Supervisor: Responsible for ensuring test procedure is followed by each of the responsible individuals, as well as for corroborating test matrix is followed.

Chapter 4: Testing and Discussion

4.1 Overview

Due to the volatile nature of kerosene, as well as its difficult handling and disposal, a decision was made to initiate experimental procedures through gas-gas (methane-oxygen) combustion. This combination has been previously employed in industry (Davis, 2004); moreover, employing different oxidizer/fuel combinations brings the advantage of adding operational parameters to the study. The methane-oxygen combustion reaction is characterized by the formula below:

$$CH_4 + 2O_2 \rightarrow CO_2 + 2H_2O \quad (32)$$

Although slightly fuel-rich conditions exist in commercial HVOF guns, it is beneficial to operate near the stoichiometric mixture ratio to ensure process efficiency and evade contamination to the coating from hydrocarbon particulates. Stoichiometric conditions imply 'ideal' combustion, meaning there is neither excess oxidizer nor excess fuel. The method for obtaining the stoichiometric O/F ratio for the methane-oxygen mixture is found below.

$$O/F = \frac{m_{oxidizer}}{m_{fuel}} = \frac{MW_{oxidizer} * Moles_{oxidizer}}{MW_{fuel} * Moles_{fuel}} = \frac{16 * 2 * 2}{(12 + 1 * 4) * 1} = 4$$

Mixtures with excess methane will have an O/F value of >4. Likewise, lean mixtures have a value greater than 4. An additional parameter employed in the characterization of a combination is defined as the oxidizer-fuel equivalence ratio, defined by equation 33. An equivalence ratio <1 falls in the range of fuel-rich combustion. An equivalence ratio >1 will

correspond to a lean, or oxidizer-rich combustion. Finally, an equivalence ratio =1 is defined as stoichiometric.

$$\lambda = \frac{{}^{O}/_{F_{actual}}}{{}^{O}/_{F_{stoichiometric}}} \tag{33}$$

4.2 Testing Procedure

All experimental investigations must follow a set test procedure. The main function of this document is ensuring the utmost operator and component safety; it also helps to certify condition repeatability. A summary of steps taken in an experimental session is detailed below. The steps below are customized for gas-gas combustion and do not include powder injection or coating. The overall process consists of three main sections: pre-testing, testing and post-testing.

Pre-testing

- Lab ventilation system is directed to nearest port for maximum disposal of gases. Range hood is activated.
- Cold flow is performed for desired testing flows as a function of line pressure.
- A leak check is executed for all lines.
- Visual inspection of the setup and lines (valves are closed, no apparent debris) performed prior to initiating recording.
- Test document is created stating all flow conditions. A space for annotations and proposed changes is marked in the document.

- Safety considerations are reviewed: automated valves opening/closing, no other personnel present in the vicinity, equipment readings accurate, hearing protection in place.

Testing

- Lines are purged using inert gas (nitrogen).
- If torch is required, hardware technician initiates combustion.
- Igniter is activated; spark existence is verified through voltage in DC supply.
- Lines are pressurized with gases.
- Simultaneous opening of the valves required for rapid mixing.
- Following 5 seconds continuous combustion, igniter is turned off and valves are closed.
- Oxidizer valve is activated for line purging.
- Fuel valve is activated for line purging.
- Valves are closed.

Following the steps above, enough time must be allowed for all unburned gases and combustion products to exit the general vicinity through the main ventilation system. If another test is required for the same conditions, testing procedure may be repeated. If different flows are required, cold flow and revision of pre-testing steps must occur. If no more tests are to be performed, proceed to post-testing procedure.

Post-Testing

- Oxygen valve is opened; tank is closed and line is allowed to depressurize
- Oxygen line is purged using inert gas and closed.

- Fuel valve is opened; fuel tank is closed and line allowed to vent gases
- Fuel line is purged and closed.
- Ventilation systems and power supplies are deactivated.
- Visual inspection of setup is performed. All valves and tanks are to be closed.

4.3 Emergency Procedure

An emergency procedure is to be implemented in the case of a misfiring, unsustainable combustion or any unwanted occurrences. The emergency procedure activates on automatic mode when redlines are reached; nevertheless, all test operators must carefully observe testing session and monitor flows for possible safety breaches. Reasons for activating emergency procedure include unwanted smoke in setup, ignition failure, software malfunction and pulsating operation.

The kill switch is hard-wired to both the ignition system as well as the injection mechanism. During normal operation the igniter is deactivated and valves are closed manually and separately; the advantage of closing these systems simultaneously lies in the fact that combustion is almost immediately stopped, as opposed to self-sustainment or possible accumulation and explosion through the deactivation of one component. The continuous burning of debris inside the chamber must be handled carefully, as re-ignition may occur. Following an emergency procedure setup, the kill switch must be reactivated through the restart of the LabView interface. Normal venting and post testing procedures are always to be followed once situation is deemed safe.

4.4 Testing Sessions

Initial

Initial testing sessions served to show flaws in setup configuration and safety operations. Following unexpected combustion through detonation and a lag in emergency procedure implementation it was decided to provide easy access to the kill switch. An operator must now always be in charge of the procedure in the event of an emergency. Coolant leaks were apparent during the first rounds of testing; although Dynalene is not a flammable material and poses no risk, gaskets were added to manage the issue and provide effective sealing. Additionally, extra Kevlar walls were positioned to supply hazard management.

The appearance of sparks during the first testing rounds served to show the importance of managing residue inside the lines and setup; when inserting seeding materials these types of issues could be critical in the ultimate output of the coating. The most acute component found to be in necessity of alteration or redesign was found to be the ignition system. Delays in combustion can cause fuel accumulation resulting in either small explosions that can come to degrade the system or in an unexpected fire outside the experimental setup. The original configuration of the igniter can be seen in the figure below. Although sparking was found to be optimal between positive and negative ports, gas mixing failed to provide a flammable region in the general area of spark location.

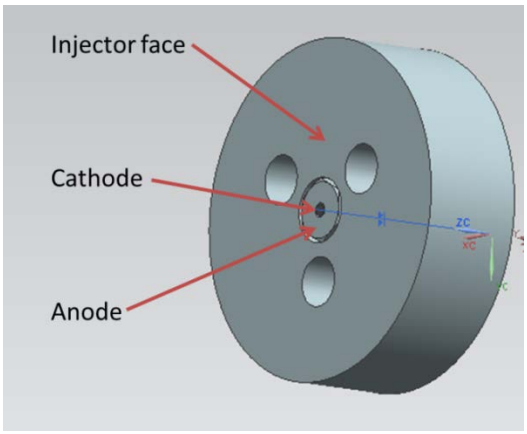

Figure 4.13: Original Ignition System

Flammability Investigation

In order to analyze the flammability limits of the mixture an initial solution was provided in the form of an external torch igniter which prevented unburned products from accumulating in the exhaust enclosure. An investigation of flame shape was performed through the intent of reaching stoichiometric O/F ratios with increasingly higher flows. An example of such tests conducted and their process conditions can be seen in Table 4.1. The overall objective of this stage was to examine flammability behavior for a methane-oxygen mixture outside of the test setup in order to analyze flame coloring and shape for a certain mixture. In these tests, oxygen flow rate was diluted in a 1:1 mixture in order to reduce flame speed and prevent flashback into the system. An O/F ratio of 4 (stoichiometric) was the norm for overall flow rates in order to examine the fuel rich to ideal combustion development. Flame investigation tests began by creating a diffusion flame, followed by the slow and controlled introduction of oxygen and nitrogen, employed to control velocity. The change in shape and color of flame was observed in order to gain knowledge of appropriate mixtures to be used inside the configuration.

Table 4.12: Flame Investigation Testing Conditions

Test #	Oxygen flow rate (slpm)	Nitrogen flow rate (slpm)	Methane flow rate (slpm)	Combustion chamber pressure (psig)	Exit Mach number	Exit Gas Velocity (m/s)
1	13	13	7	.5	.25	275.6
2	26	26	13	1.0	.35	386.4

The images below show the evolution of a flame using low flow rates as compared to industrial processes (values are those from test #1). An initial diffusion flame gives place to a premixed cone finally resulting in flashback when the mixture becomes too lean. Flame transitions from yellow/orange to light blue depending on the amount of oxygen present and the products released into the atmosphere. It is worth noting that flame temperature varies through this parameter as well; the highest achievable flame temperature exists in stoichiometric mixtures.

Figure 4.14: Rich to Lean Flame Development

Due to the previously mentioned issues with ignition several attempts to anchor the flame inside the combustion chamber were made. Controlled flashback through the addition of nitrogen was performed in order to bring combustion to the intended mixing point. Though effective for certain flows (most specifically those with lowest values), it was apparent that its continuous use can damage the system and is thus not recommended; most times, the force of flashback resulted in a blowout. The images below show successful attempts of controlled flashback performed with flows corresponding to tests #1 and #2. Final O/F ratio is close to stoichiometric, hence the blue flames; most if not all fuel is burned in the process. Exit gas velocities are calculated to be 275.6 and 386.4 m/s. The incremental values in overall flow rates result in larger plume sizes. The configuration has such been repeated in latter experiments with higher flows and different, more effective ignition systems.

Figure 4.15: Flow Rate Flame Comparison

Igniter Configuration Testing

The resolution of ignition issues is critical in the designed HVOF structure to ensure utmost safety of system components and operators. Detonation lags and/or failure can result in the accumulation of hazardous gases that, once met with a spark, result in flare-ups that can damage the system or cause a fire inside the laboratory. Several ignition locations and configurations have been proposed and tested for the system.

In all proposed configurations a rare earth tungsten rod acts as a conductor for the spark; this material has been chosen due to its record of use in similar laboratory systems and high melting temperature (3400 C vs. 1500 C in stainless steel). Rod dimensions and diameter are dependent on desired geometry. A low-current high-voltage spark is generated through a transformer, in turn activated remotely by the DC power supply. Spark location, power and length are determined by the location and material of cathode and anode. In currently tested arrangements the cathode has always been established as the main tungsten rod protected by a ceramic enclosure. Following failure of the initial igniter setup four configurations have been installed and experimented upon for equivalent flow conditions. These are outlined in Table 4.2.

Table 4.13: Igniter Configurations

Single tungsten rod protected by ceramic, arching with converging section of the nozzle	Single tungsten rod protected by ceramic, slightly bent to arc with combustion chamber wall
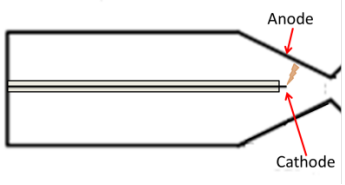	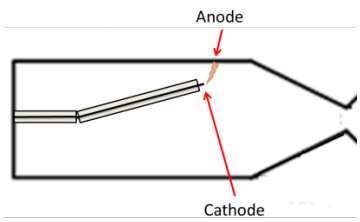
Parallel tungsten rods sparking between each other. Spark location is at the end of the combustion chamber	Parallel tungsten rods sparking between each other. Spark location is located in converging-diverging section
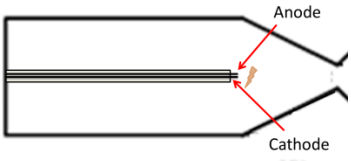	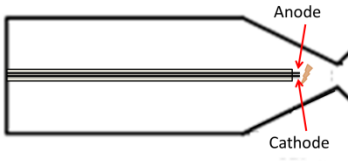

Table 4.14: Testing Conditions Employed During Ignition Investigation

Test #	Oxygen flow rate (slpm)	Methane flow rate (slpm)	Combustion chamber pressure (psig)	Exit Mach number	Exit Gas Velocity (m/s)
1	157	84	6	.8	880

Those configurations employing a spark between the body of the gun and tungsten rod have proven to be most effective in terms of instantaneous or near-instantaneous ignition, demonstrated by video evidence. Although no significant explosions were observed upon ignition, flame coloring was changed due to the failure and erosion of the tungsten rod. Once combustion was halted white smoke could be perceived as emanating from within the setup (Figure 4.4, left); at times, still-burning materials are present posing a re-ignition risk for unburned gases. Upon investigation tungsten oxide is apparent inside the gun configuration in the form of a white/yellow powder. The obvious downside of the oxidation of the igniter formation lies in the fact that coating development is highly affected by external particles and debris; additionally, a one-time use is not usually acceptable in HVOF configurations.

Figure 4.16: Observable Damage by Tungsten Rod Erosion

Configurations employing a smaller spark generated between two tungsten rods presented ignition delays varying between 3 and 5 seconds, generating small explosions upon combustion initiation. Although not alarming at these flow rates, an ignition delay with significantly higher flows may affect the configuration or cause dangerous conditions. Although spark location has been changed, an investigation of delay as a function of location must be performed in order to accept this as a final solution to ignition. It is worth noting however that the force of ignition has caused and can be the cause in the future for blowout due to the expanding nature of the gases when coming in contact with the spark. Those igniters tested close to the converging section of the nozzle presented the most damage due to the highest generated temperatures in the system. Placement should look for earliest mixing point in order for the igniter to suffer the least amount of damage. Alternate ignition solutions must be actively sought out in order to optimize the system.

The flame generated using the flow rates described in Table 4.3 can be seen in the Figure below. As opposed to flame investigation experiments a non-stoichiometric ratio (3.5) was chosen due to industrial HVOF guns operating in slightly rich conditions. An example of such a process can be seen in the right. Flame shape appears to be similar but rounded in the case of the experimental figure; this is due to lower flow rates employed resulting in lesser velocities and overall smaller energies. Higher flow rates and an improved control of mixing times will be employed to compare the current setup with existing data.

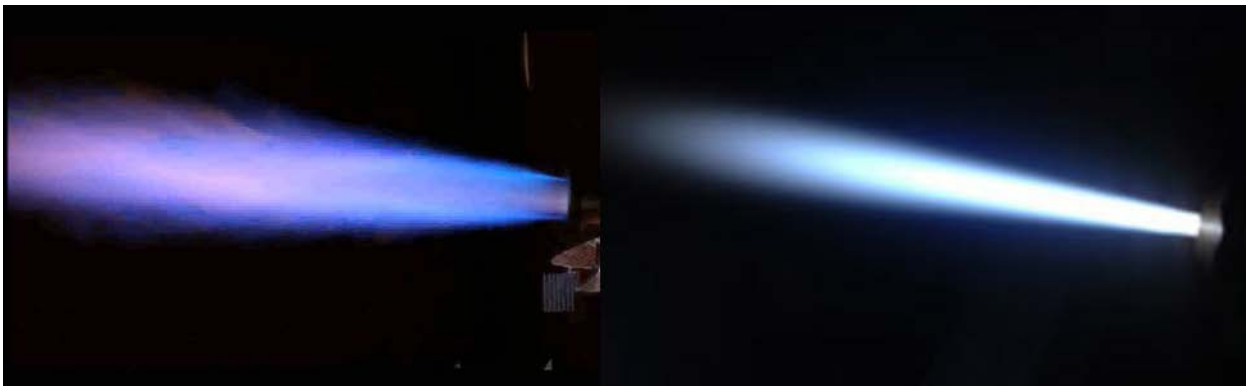

Figure 4.17: Actual vs. Industrial HVOF Flame Comparison

Chapter 5: Computational Modeling

5.1 Review and Conditioning

A fundamental understanding of all processes such as gas dynamic properties and particle behavior cannot be obtained solely by an experimental approach. The modelling and simulation of HVOF processes is of utmost importance to further optimize real-life designs (Dongmo, Wenzelburger, & Gadow, 2008). Computational modeling is difficult due to the fact that several conditions must be taken into account and coupled i.e. premixed combustion, turbulent multi-component flow, multiphase flow (if the fuel is liquid), compressible and subsonic/supersonic reacting flow (Dongmo, Wenzelburger, & Gadow, 2008). Numerical models have been previously defined and studied in various investigations as noted above, namely by Gu (Kamnis & Gu, 2006) (Tabbara & Gu, 2009), Kamali (Kamali & Binesh, 2009), Dongmo (Dongmo, Wenzelburger, & Gadow, 2008) and Basu (Basu & Cetegen, 2008). Most of these studies focus heavily on the internal combustion characteristics of the gun and fuel atomization rather than external jet characteristics.

Gu (Kamnis & Gu, 2006) focused on comparing computational and experimental results in terms of temperature as a function of radial distance. An experimental approach to this result type can be done through the use of internal thermocouples to analyze thermal gradients. This investigation deals with the atomization and vaporization of a kerosene-fuelled gun; it is mentioned that the combustion process is highly dependent on initial fuel droplet sizes as well as recirculation flows (Kamnis & Gu, 2006). This study also found that the core of a flame is stretched by droplets with larger sizes, and that fuel droplets greater than 5 μm might combust outside of the C-D nozzle, reducing overall temperature and contaminating the powder. A

computational investigation of droplet injection and atomization will be done previous to developing the liquid-section of the experimental setup. For future studies, parameters such as fuel injection angle and type can be changed; additionally, an external heat source prior to injection can be added to the setup in order to study the partial vaporization of kerosene.

The model presented in this investigation is simplified in 2-d due to the large computational resources that this would otherwise require. The obvious downside of a simple scheme is the fact that the injection geometry's influence on combustion cannot be analyzed; rather, simple injection boundary conditions are to be defined. However, since a steady-state model is employed overall results (such as temperature, chamber pressure, etc.) should not differ much from different injection models.

The model consists of four main components (injector, combustion chamber, c-d nozzle, barrel) based on gun geometry parameters. A methane-oxygen configuration was chosen for similar reasons as in the experimental section of the study. An additional free space has been added to study the jet's behavior outside the gun. The overall geometrical schematic can be seen in the following figure, along with its contours of cell volume which show smaller cells are concentrated in the actual setup geometry; the grid is represented by the means of this image showing highest existing density in the centerline. A mesh independence test has been previously performed through an overall change in mesh coarseness and result analysis.

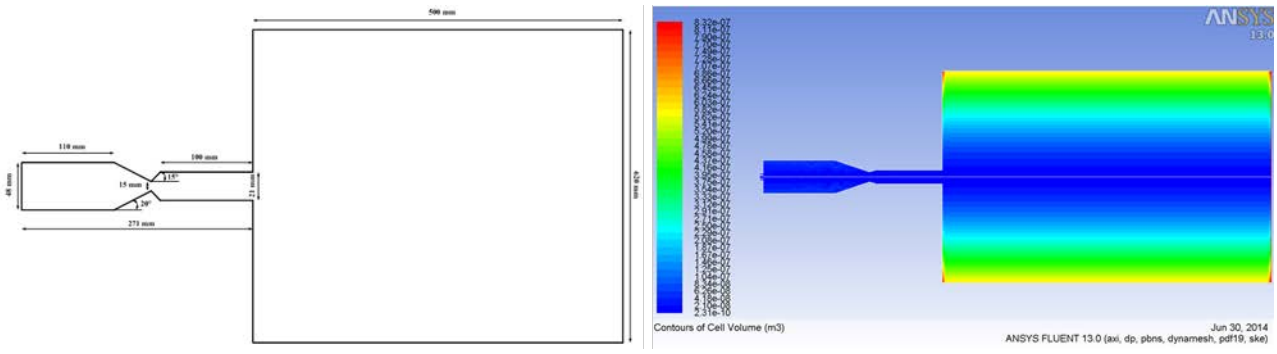

Figure 5.18: Sizing and Contours of Cell Volume for Computational Model

CFD calculations were performed using ANSYS Fluent 6.3, solving conservation equations of mass, momentum, energy and species reactions. A realizable k –ε model was employed to simulate the turbulent flow field. This turbulence model is usually employed in these simulations due to the high values of Reynolds numbers present as well as the pressure gradients found in the combustion chamber and nozzle geometries (Dongmo, Wenzelburger, & Gadow, 2008).

Working conditions are established in Table 5.1. Three overall oxygen flow rates were considered; methane flow rates were determined according to three O/F ratios. High volumes of oxygen were chosen due to the desire to investigate supersonic conditions for the geometrical configuration, as that is defined as the ultimate purpose of the setup. Key process parameters are then established as total flow rate and equivalence ratio. Equivalence ratios are defined as lean (.9), stoichiometric (1) and rich (1.1) to investigate how pressure and temperatures are affected through their change. Inlet temperatures are set through the initial conditions of the model to be 300 K. Interior gun surfaces are assumed to be cooled by a constant temperature boundary condition (350 K). Actual gun cooling can be further investigated through a different geometrical setup. External boundary conditions are set to be 300 K and 1.013×10^5 Pa.

Table 5.15: Summary of Employed Conditions

Case	Oxygen mass flow rate, g/s	Fuel mass flow rate, g/s		
		Equivalence ratio = 0.9	Equivalence ratio = 1.0	Equivalence ratio = 1.1
A	20	4.5	5	5.6
B	25	5.6	6.3	6.9
C	30	6.7	7.5	8.3

The numerical method used for the convergence of the solution is a coupled algorithm with a finite-volume assumption. A coupled solution was chosen due to the fact that convergence problems due to oscillations in pressure and velocity fields can be avoided (Kamali & Binesh, 2009). It is also more stable and economical on computational resources when compared to other algorithms. A second order upwind scheme is employed for the discretization of the model, after a first-upwind solution has been converged, similar to methods found in literature (Li & Christofides, 2005). It provides stability for the pressure correction equation. Combustion models are varied in the software. A non-premixed combustion approach was chosen due to its simplicity as compared to others; a template within the program establishes reactions thus simplifying the work of the user, who only has to appropriately choose boundary conditions. The non-premixed approach follows the complete chemical reaction approach for methane-oxygen combustion, described in chapter 3.Heat transfer through radiation can be approximated by the P1 model which assumes that radiation intensity is isotropic or direction independent for a given location. A brief overview of employed boundary conditions and models follows below. Governing equations for the turbulence and combustion models can be found in the literature provided by Gu (Kamnis & Gu, 2006), Dongmo (Dongmo, Wenzelburger, & Gadow, 2008) and Li (Li & Christofides, 2005).

Model/Boundary Condition	Denomination
Turbulence	k –ε (realizable)
Combustion	non-premixed
Cooling	Constant Wall Temperature
Radiation	P1
Inlets	Mass Flow
Outlet	Atmospheric Pressure Condition
Convergence Criteria	Second Order Upwind

5.2 Results

A sample result for an axial temperature plume contour is shown in the figure below; experimental result is shown on the right. It is apparent that the highest combustion temperature is reached at the throat, with an almost constant value up until the jet exits into the atmosphere. A cold central temperature in the combustion chamber can be attributed to the initial boundary condition of 300 K for oxygen as well as the velocity disparity. Proper mixing does not occur until the beginning of the converging section.

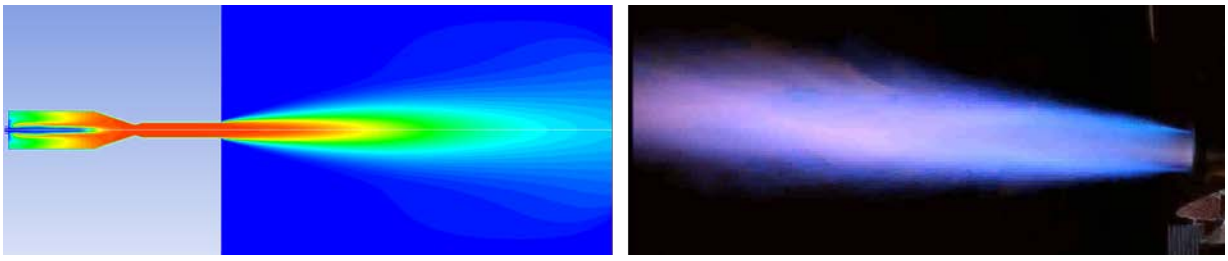

Figure 5.19: Contours Temperature Comparisons for Computational and Experimental Plumes

Results corresponding to Mach number according to both increasing flow and equivalence ratio are shown below. It can be observed from the images that supersonic

conditions are always reached at the nozzle throat; a slightly rich equivalence ratio yields the highest Mach number (around 1.9), while a lean mixture corresponds to the lowest values. Similarly, Mach number is directly proportional to overall flow as seen on the right side.

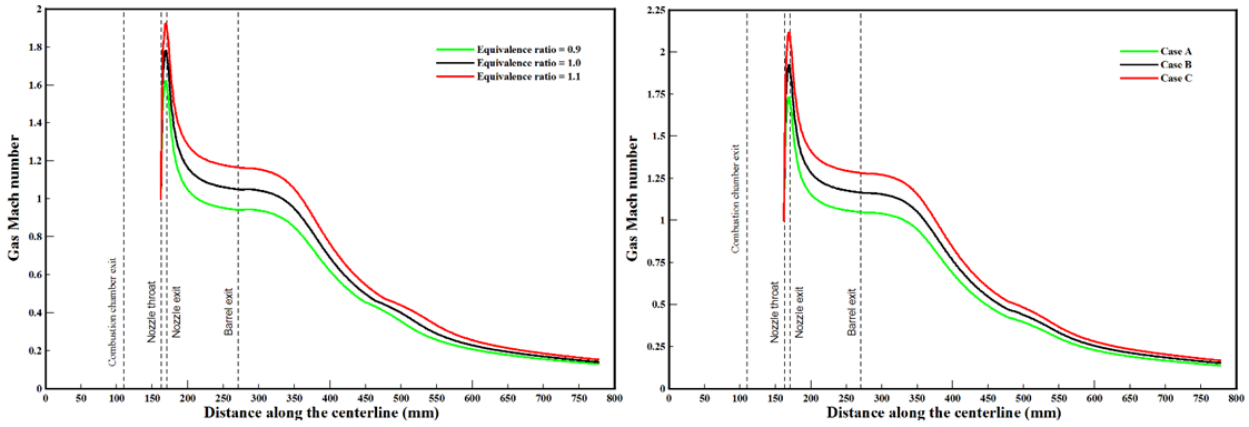

Figure 5.20: Mach Number Contours as a function of Equivalence Ratio and Overall Flow

The contours of gas static pressure as a function of centerline distance are viewed in figure 5.4. In a similar computational investigation Kamali et al. found that the pressure remains high in the combustion chamber, decreases sharply in the CD nozzle and reaches near atmospheric level in the barrel section. This is consistent with results obtained for the configurations investigated; while slight pressure fluctuations are found in the combustion chamber, once the throat is reached pressure sharply decreases. All investigated points reach near-atmospheric pressure with high velocities. As see in Figure 5.4, a rich configuration with the highest flow rate will yield the highest combustion chamber pressure. Appreciated in Figure 5.5 is the fact that axial velocity is inversely proportional to gas pressure, corresponding to the energy conversion mechanism occurring in the nozzle section. This figure also shows that either a slightly rich configuration or a larger flow rate will result in higher velocities.

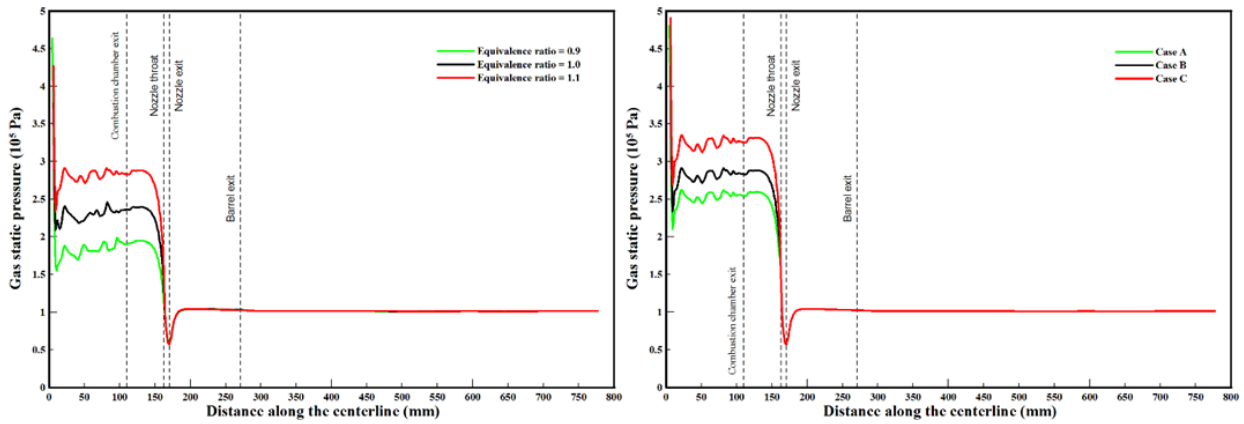

Figure 5.21: Gas pressure Values as a Function of Equivalence Ratio and Overall Flow

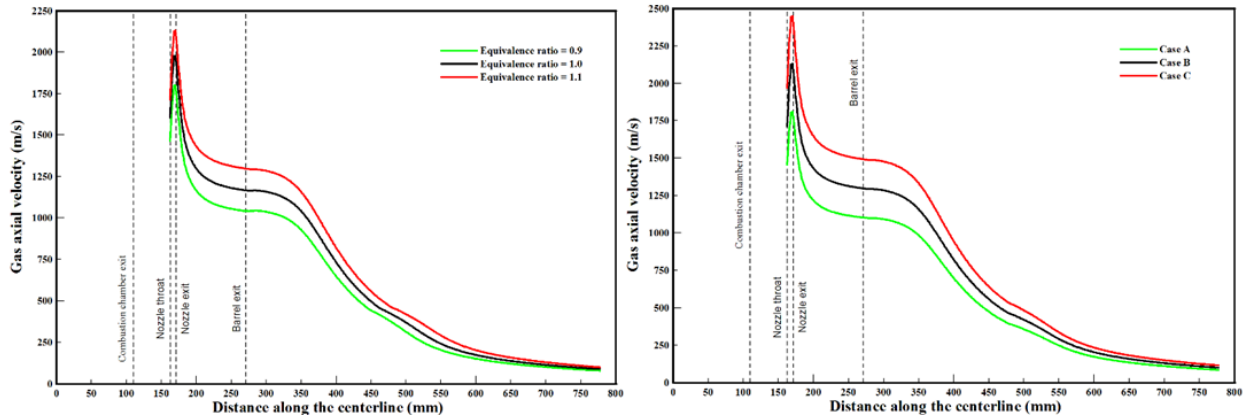

Figure 5.22: Velocity Values as a Function of Equivalence Ratio and Overall Flow

Future computational investigations as related to the project can be performed using transient conditions, in order to observe how ignition source and type, along with injector geometry affect flame development. There is also an interest in employing the eddy dissipation model (EDM) as various works of literature cite it, such as that one performed by Li et. Al. This model assumes the reaction rate is limited by turbulent mixing rate and models chemistry reaction. Although an initial EDM model was performed for this study, the non-premixed combustion model proved to have increased accuracy, particularly in the temperature investigation. This can be explained by the fact that as temperature increases above 2000 K CO2 and H2O will dissociate into a number of species with low molecular weight due to strong

thermal atomic vibration. Studies have shown that a combustion model which does not account for the dissociation of combustion products will over predict the combustion temperature (Li & Christofides, 2005); initial computational modeling overestimated this value by over 2000 K. Additional requirements for further investigations include a complete cooling heat transfer system as well as particle injection simulations to set appropriate flow values in the experimental setup.

Chapter 6: Conclusions and Future Work

A liquid based HVOF configuration has been developed according to rocket design guidelines. Design was manufactured and assembled with flow monitoring and regulating instrumentation. Setup behavior and flammability ranges have been investigated for a methane-oxygen mixture. Testing revealed initial flaws in lines and remote monitoring arrangements; adequate steps have been taken for the continuous improvement of setup and procedure. Successful tests have shown similar flame shape and oxygen-fuel mixing conditions to industrial HVOF systems with varying exit velocities and overall flow rates. Due to a much different throat diameter from standardized configurations relatively higher gas flows will be required to reach desired particle kinetic and thermal energies. A maximum safe combustion lag is to be determined based on increasing gas rates; if available, different ignition systems are to be experimented upon to minimize this risk. Gas-gas combustion is to be continued until desired rates are achieved; upon this point particle injection and coating formation will commence. The inclusion of a computational chapter has aided in the understanding of pressure-velocity exchange mechanisms for designed geometry. Future work objectives for the project are as follows:

In-flight particle diagnosis

Since the kinetic energies of particles can influence characteristics of the coating (i.e. adhesive strength, density, young's modulus and roughness) it is important to examine them through different means. A determination of the relationship between particle velocity and the mentioned parameters can help researchers obtain increased understanding of sprayed coating properties (Bach, Mohwald, Engl, Drobler, & Hartz, 2006). On site laser/optical diagnostic techniques such

as high speed stereo particle image velocimetry (PIV) and high speed two color pyrometry will be used to monitor flux distributions, velocity, and temperature of particles. The quantification of these parameters is necessary in order to relate them to final coating characteristics.

With particle image velocimetry thermal spraying processes can be effectively visualized due to the size of the measuring area, typically in a range of several square centimeters. In PIV flying particles are illuminated by two laser flashes following each other in quick sequence. The light is detected by a camera placed orthogonally. The system can either take two images (for each laser flash) or one double-exposed image of these. When analyzing images each particle will appear as a particle image pair. According to the distance between these, identified time difference between laser pulses and the direction of the flying particles, it's likely to calculate the magnitude and direction of the vector for individual particles. PIV involves an extensive range of methods for the determination of image-particle relationship. It is not suitable however for high particle densities (Bach, Mohwald, Engl, Drobler, & Hartz, 2006).

In-depth Computational Investigation

Although the basis for boundary conditions in an HVOF system has been explored in the computational section of the study, no real circumstances have been evaluated as the supersonic threshold has not yet been reached experimentally. Once sufficiently high flows have been reached in the structure an accurate computational/experimental comparison may be performed. A contrast of combustion models is particularly desired (e.g. eddy dissipation vs. premixed) due to few studies focusing on this aspect; 2d vs 3d models can also be employed to shed light on the influence of injector geometry on combustion mechanisms. Particle injection simulation into the stream is a supplementary concept that has the potential to further enlighten the current study.

Once the transition into liquid for the system is fully complete, droplet injection parameters and rates of evaporation can be investigated to determine parameters to be changed in the case of incomplete combustion and/or too-large droplets.

Investigation of coating mechanical and chemical properties

The quantification of test parameters is an important overall objective in the research study. Generated coating properties such as residual stress, oxidant content and density are to be investigated using x-ray diffraction and SEM technology, along with fatigue and fracture testing procedures. Initial coatings are to be composed of FeAl particles using the current gas-gas gun configuration; the gas-gas arrangement coatings will be compared to liquid-gas combination results once the transition has been made. Latter studies will employ Inconel 718 particles for bond coat composition.

Continuous setup improvement and transition into liquid

As evidenced in the conclusions, the testing setup must be always in the process of redesigning and reconfiguring to achieve the optimal operation of the experimental procedure. Although only one parameter must be changed per objective to properly correlate results with variations, the setup is expected to be able to alter one mechanism at a time until a completely new design is obtained. Since the overall project has been planned with liquid-gas combustion in mind a transition must be performed sometime in the future in order to fulfill the requirement. Finally, a system redesign may be able to take place to accommodate components that cannot be integrated in the current setup (internal thermocouples, pressure sensing device inside the combustion chamber) and/or fulfill a different design approach.

References

Bach, F., Mohwald, K., Engl, L., Drobler, E., & Hartz, K. (2006). Particle Image Velocimetry in Thermal Spraying. *Advanced Engineering Materials*, 650-653.

Basu, S., & Cetegen, B. M. (2008). Modeling of liquid ceramic precursor droplets in a high velocity oxy-fuel flame jet. *Acta Materialia, 56*, 2750-2759.

Brandl, W., Toma, D., Kruger, J., Grabke, H., & Matthaus, G. (1997). The oxidation behaviour of HVOF thermal-sprayed MCrAlY coatings. *Surface & Coatings Technology*, 21-26.

Clarke, D., & Phillpot, S. (2005). Thermal barrier coating materials. *Materials today*, 22-29.

Davis, J. R. (2004). *Handbook of Thermal Spray Technology.* ASM International.

Dongmo, E., Wenzelburger, M., & Gadow, R. (2008). Analysis and optimization of the HVOF process by combined experimental and numerical approaches. *Surface & Coatings Technology*, 4470-4478.

Dynalene Company. (n.d.). Retrieved from Dynalene Selection Guide: www.dynalene.com/Fluid-selection-guide-s/1828.htm

Huzel, D. K., & Huang, D. H. (1992). *Modern Engineering for Design of Liquid Propellant Rocket Engines.*

Ibrahim, E. A., Kenny, R. J., & Walker, N. B. (2010). Atomization of Shear Coaxial Liquid Jets. *Applied Physics Research*.

Jang, H., Park, D., Jung, Y., Jang, J., Choi, S., & Paik, U. (2006). Mechanical characterization and thermal behavior of HVOF-sprayed bond coat in thermal barrier coatings (TBCs). *Surfaace & Coatings Technology, 200*, 4355-4362.

Kamali, R., & Binesh, A. (2009). The importance of sensitive parameters effect on the combustion in a high velocity oxygen-fuel spray system. *International Communications in Heat and Mass Transfer*, 978-983.

Kamnis, S., & Gu, S. (2006). 3-D Modelling of kerosene-fuelled HVOF thermal spray gun. *Chemical Engineering Science*, 5427-5439.

Kamnis, S., & Gu, S. (2006). Numerical modelling of propane combustion in a high velocity oxygen-fuel thermal spray gun. *Chemical Engineering and Processing*, 246-253.

Katanoda, H., Morita, H., Komatsu, M., & Kuroda, S. (2011). Experimental and Numerical Evaluation of the Performance of Supersonic Two-Stage High-Velocity Oxy-Fuel Thermal Spray (Warm Spray) Gun. *Journal of Thermal Science*, *20*(1), 88-92.

Li, M., & Christofides, P. (2005). Multi-scale modeling and analysis of an industrial HVOF thermal spray process. *Chemical Engineering Science*, 3649-3669.

Li, M., & Christofides, P. (2005). Multi-scale Modeling and Analysis of an Industrial HVOF thermal Spray Process. *Chemical Engineering Science, 60*, 3649-3669.

Mohamed, D., Cabrera, L., Love, N., & Choudhuri, A. (2014). High Velocity Oxy-Fuel Thermal Spray Gun Design. *AIAA SciTech 2014.* Baltimore.

Pyroblanket 32oz. (n.d.). Retrieved 08 01, 2014, from Insuflex: http://adlinsulflex.com/fire-blankets/pyroblanket-32-oz/

Salgues, D., Mouis, G., Lee, S. Y., Kalitan, D. M., Pal, S., & Santoro, R. (2006). Shear and Swirl Coaxial Injector Studies of the LOX/GCH4 Rocket Combustion Using Non-Intrusive Laser Diagnostics. *44th AIAA Aerospace Sciences Meeting.*

Singh Nalwa, H. (1999). *Handbook of Nanostructured Materials and Nanotechnology*. Academic Press.

Sutton, G. (2005). *History of Liquid Propellant Rocket Engines.*

Sutton, G. P., & Biblarz, O. (2010). *Rocket Propulsion Elements.*

Tabbara, H., & Gu, S. (2009). Computational Simulation of liquid-fuelled HVOF thermal spraying. *Surface & Coatings Technology*, 676-684.

Yang, V., Habiballah, M., Popp, M., & Hulka, J. (2005). *Liquid Rocket Thrust Chambers.*

Glossary
(In Order of Appearance)

D_t	Throat Diameter	ΔP_o	Injector Pressure Drop in Oxidizer Line
P_c	Chamber Pressure	ρ_f	Fuel Density (Kerosene)
γ	Specific Heat ratio	$\rho_{o@atm}$	Oxidizer Density
g	Gravitational acceleration	t_o	Thickness of Oxidizer Post
$\bar{R}$	Adapted Universal Gas Constant	P_f	Fuel Line Pressure
M_{wt}	Molecular Weight of Gases	P_o	Oxidizer Line Pressure
T_c	Combustion Chamber Temperature	D_{oi}	Oxidizer Orifice Inner Diameter
		D_{oo}	Oxidizer Orifice Outer Diameter
O/F	Oxygen to Fuel Ratio	D_f	Fuel Orifice Diameter
A_t	Throat Area	A_t	Throat Area
R	Gas Constant	L_c	Combustion chamber length
$\dot{m}_t$	Total Gas Flow Rate	D_c	Combustion chamber diameter
$\dot{m}_o$	Oxygen Mass Flow Rate	A_c	Combustion chamber area
$\dot{m}_f$	Fuel Mass Flow Rate	S	Allowable working stress of chamber material
N	Number of orifices		
C_d	Dimensionless Discharge	V_c	Combustion chamber volume
ΔP_f	Injector Pressure Drop in Fuel Line	L^*	Characteristic chamber length
		t_w	Chamber wall thickness

β	Converging half-angle
α	Diverging half-angle
T_c	Combustion chamber temperature
γ	Specific heat ratio
P_c	Combustion chamber pressure
P_{atm}	Atmospheric pressure
T_t	Throat Temperature
P_t	Throat Pressure
M_{a_e}	Exit Mach Number
V_e	Exit Velocity
T_e	Exit Temperature
D_e	Exit Diameter
NPR	Nozzle Pressure Ratio
L_{barrel}	Barrel Section Length
D_{barrel}	Barrel Section Diameter
q	Average HVOF heat transfer rate
$C_{p_{coolant}}$	Coolant heat capacity
A_{total}	Setup Area to be cooled
Q_{total}	Total Heat Transferred
D_i	Theoretical cooling jacket inner diameter
D_c	Theoretical cooling jacket outer diameter

Vita

Luisa Cabrera was born in Chihuahua, Mexico on June 4, 1990, the daughter of Luis Cabrera and Aurora Maynez. After completing her high school studies at Tecnologico de Monterrey in Ciudad Juarez she went on to study at The University of Texas at El Paso, graduating with honors and receiving her bachelor's in Mechanical Engineering in December 2012. She entered the Master's program at the same university the following semester, initiating herself in the fields of research and teaching. In the future, Luisa hopes to obtain a doctoral degree and pursue an academic career in the field.

Permanent address: 4750-6 Palma Areca
Paseo de las Palmas
Cd. Juarez, Chihuahua, Mexico 32664

This thesis/dissertation was typed by the author.